The wobbling mode in A ~ 130 nuclei

C.M. Petrache
University Paris-Sud & CSNSM Orsay
(Centre de Sciences Nucléaires et Sciences de la Matière)

1. Wobbling in Lu-Ta nuclei
2. Transverse wobbling in ^{135}Pr
3. Transverse wobbling in ^{138}Nd
4. Future plans and perspectives

VOLUME 86, NUMBER 26 PHYSICAL REVIEW LETTERS 25 JUNE 2001

Evidence for the Wobbling Mode in Nuclei

S. W. Ødegård,[1,2] G. B. Hagemann,[1] D. R. Jensen,[1] M. Bergström,[1] B. Herskind,[1] G. Sletten,[1] S. Törmänen,[1] J. N. Wilson,[1] P. O. Tjøm,[2] I. Hamamoto,[3] K. Spohr,[4] H. Hübel,[5] A. Görgen,[5] G. Schönwasser,[5] A. Bracco,[6] S. Leoni,[6] A. Maj,[7] C. M. Petrache,[8,*] P. Bednarczyk,[7,9] and D. Curien[9]

^{163}Lu

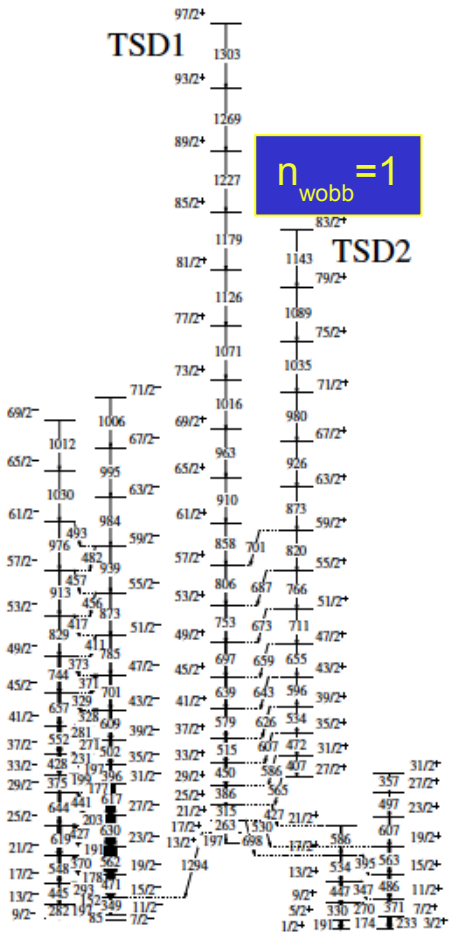

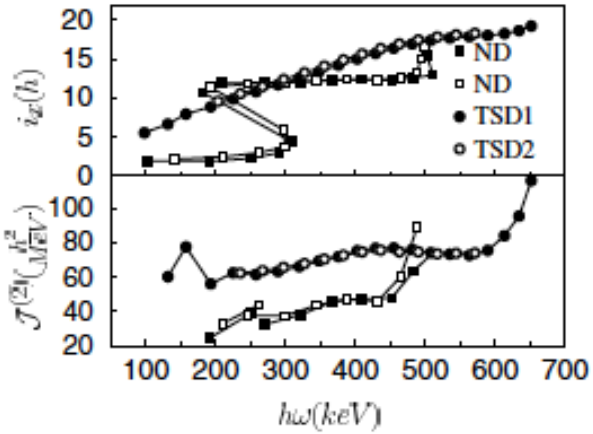

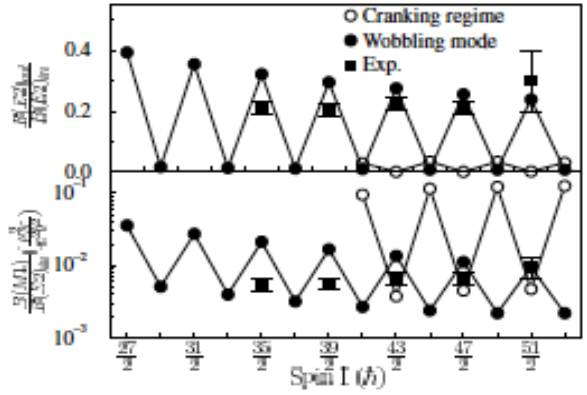

TABLE I. Experimental and calculated values of mixing ratio δ, branching ratio λ, and electromagnetic nature of the connecting transition for $I = 43/2\hbar \rightarrow I = 41/2\hbar$.

	δ	λ	E/M
Expt.	$-3.10^{+0.36}_{-0.44}$	0.36 ± 0.04	E
Wobbling	-2.4^{a}	0.48^{a}	E
Crankinglike	$\pm 0.15^{a,b}$	0.02^{a}	M

VOLUME 89, NUMBER 14 PHYSICAL REVIEW LETTERS 30 SEPTEMBER 2002

Evidence for Second-Phonon Nuclear Wobbling

D. R. Jensen,[1] G. B. Hagemann,[1] I. Hamamoto,[1,2] S. W. Ødegård,[1,3] B. Herskind,[1] G. Sletten,[1] J. N. Wilson,[1] K. Spohr,[4] H. Hübel,[5] P. Bringel,[5] A. Neußer,[5] G. Schönwaßer,[5] A. K. Singh,[5] W. C. Ma,[6] H. Amro,[6] A. Bracco,[7] S. Leoni,[7] G. Benzoni,[7] A. Maj,[8] C. M. Petrache,[9,10] G. Lo Bianco,[10] P. Bednarczyk,[8,11] and D. Curien[11]

^{163}Lu

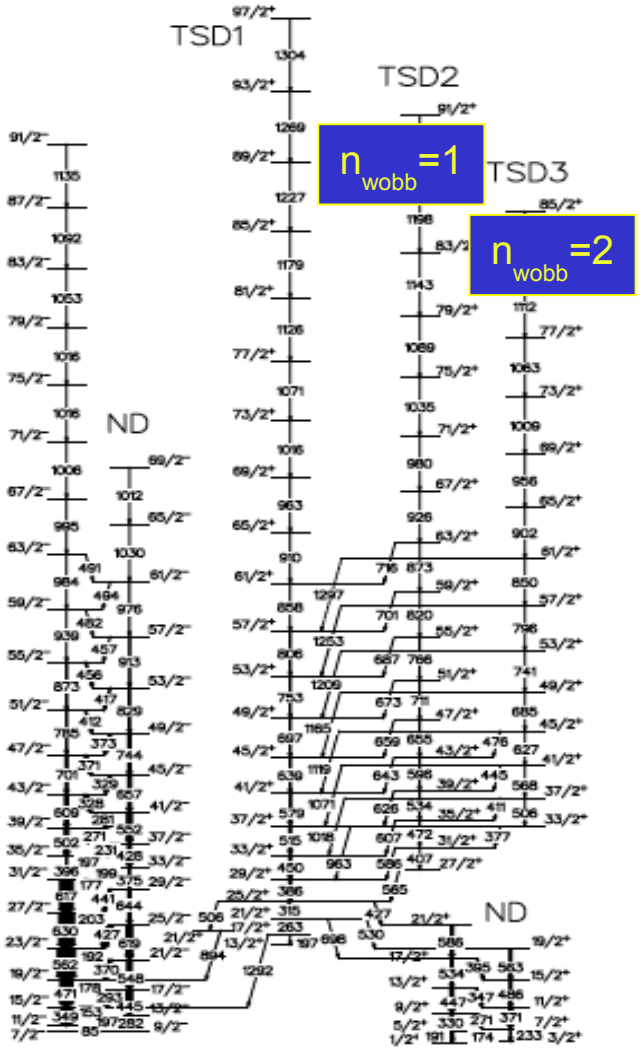

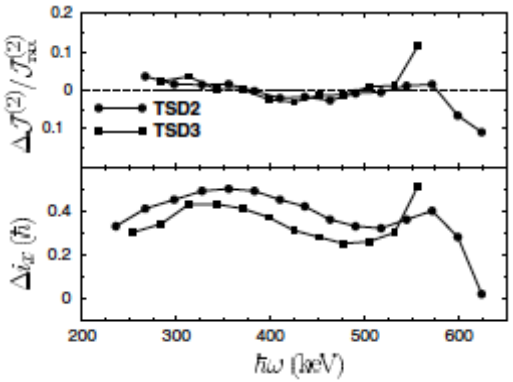

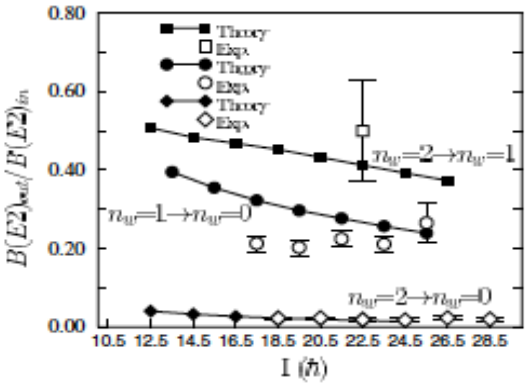

TABLE II. Experimental values of branching ratio λ, angular distribution ratio $W(25°)/W(90°)$, DCO ratio, mixing ratio δ, and $B(E2)_{out}/B(E2)_{in}$ for $\Delta I = 1\hbar$ transitions. Upper part: The 476 keV transition from TSD3 to TSD2. Lower part: Average values for transitions from TSD2 to TSD1.

λ	$\frac{W(25°)}{W(90°)}$	DCO-ratio[a]	$\langle\delta\rangle$	$\frac{B(E2)_{out}}{B(E2)_{in}}$
0.14 ± 0.04	0.49 ± 0.10	0.38 ± 0.11	$-3.60^{+0.97}_{-1.93}$	0.51 ± 0.13
...	...	...	$-0.19^{+0.08}_{-0.12}$	$0.019^{+0.024}_{-0.017}$
	0.46 ± 0.05	0.33 ± 0.03	$-3.10^{+0.36}_{-0.44}$	0.21 ± 0.01

^{165}Lu

One- and two-phonon wobbling excitations in triaxial ^{165}Lu

G. Schönwaßer [a], H. Hübel [a], G.B. Hagemann [b], P. Bednarczyk [c,d], G. Benzoni [e], A. Bracco [e], P. Bringel [a], R. Chapman [f], D. Curien [c], J. Domscheit [a], B. Herskind [b], D.R. Jensen [b], S. Leoni [e], G. Lo Bianco [g], W.C. Ma [h], A. Maj [d], A. Neußer [a], S.W. Ødegård [i], C.M. Petrache [g], D. Roßbach [a], H. Ryde [j], K.H. Spohr [f], A.K. Singh [a]

Physics Letters B 552 (2003) 9–16

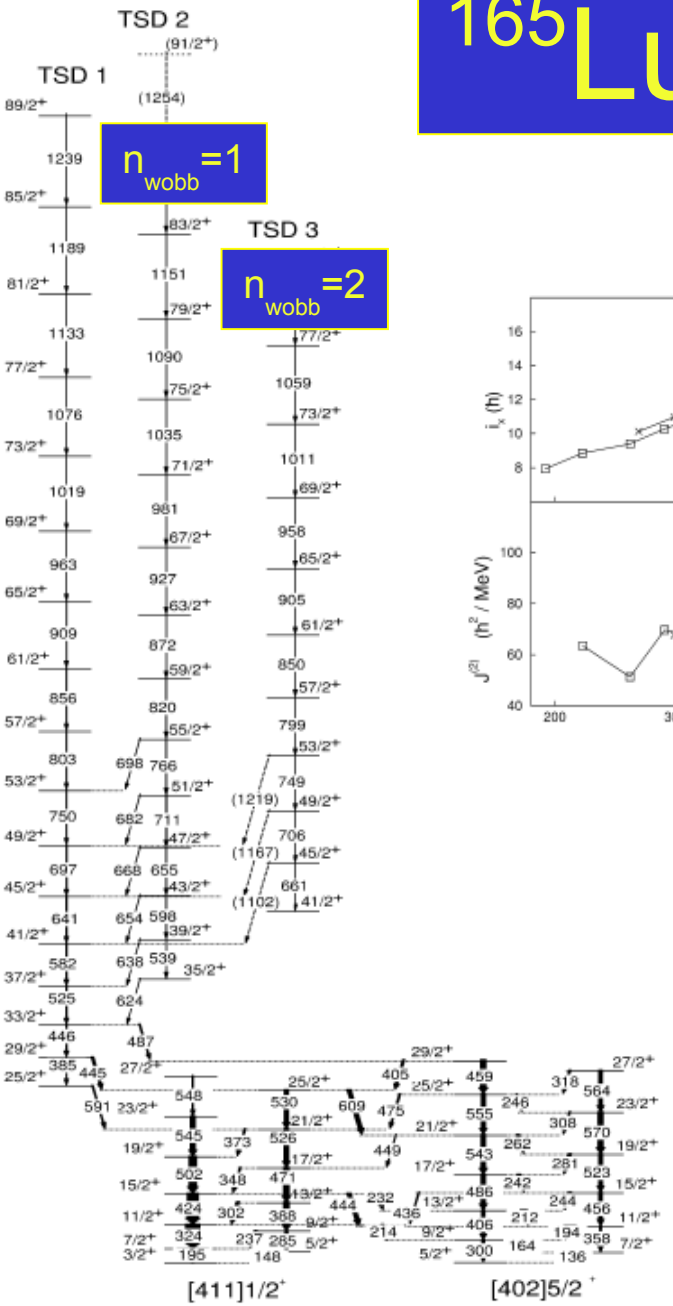

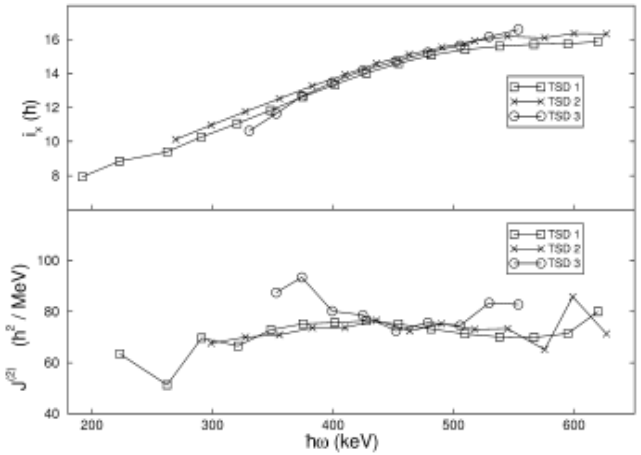

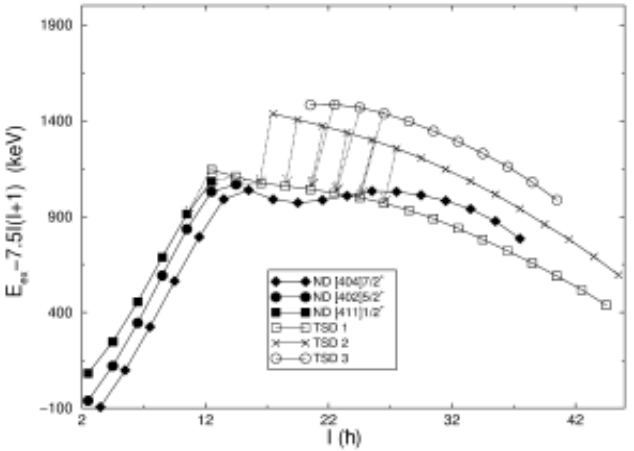

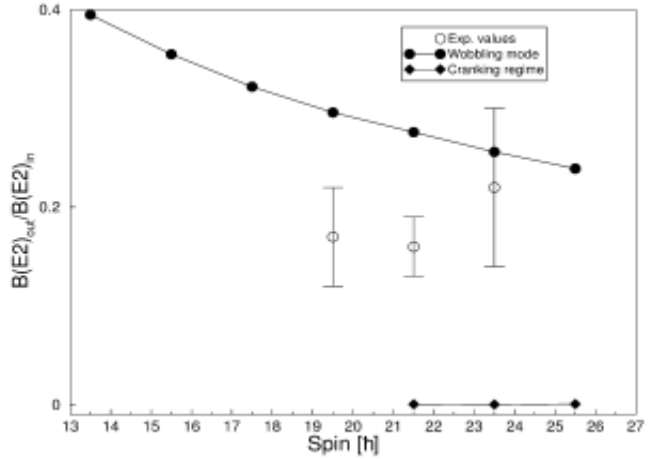

PHYSICAL REVIEW C 80, 041304(R) (2009)

Wobbling mode in ^{167}Ta

D. J. Hartley,[1] R. V. F. Janssens,[2] L. L. Riedinger,[3] M. A. Riley,[4] A. Aguilar,[4,*] M. P. Carpenter,[2] C. J. Chiara,[2,5,6] P. Chowdhury,[7] I. G. Darby,[3] U. Garg,[8] Q. A. Ijaz,[9] F. G. Kondev,[5] S. Lakshmi,[7] T. Lauritsen,[2] A. Ludington,[1,†] W. C. Ma,[9] E. A. McCutchan,[2] S. Mukhopadhyay,[8] R. Pifer,[1] E. P. Seyfried,[1] I. Stefanescu,[2,6] S. K. Tandel,[7] U. Tandel,[7] J. R. Vanhoy,[1] X. Wang,[4] S. Zhu,[2] I. Hamamoto,[10] and S. Frauendorf[8]

^{167}Ta

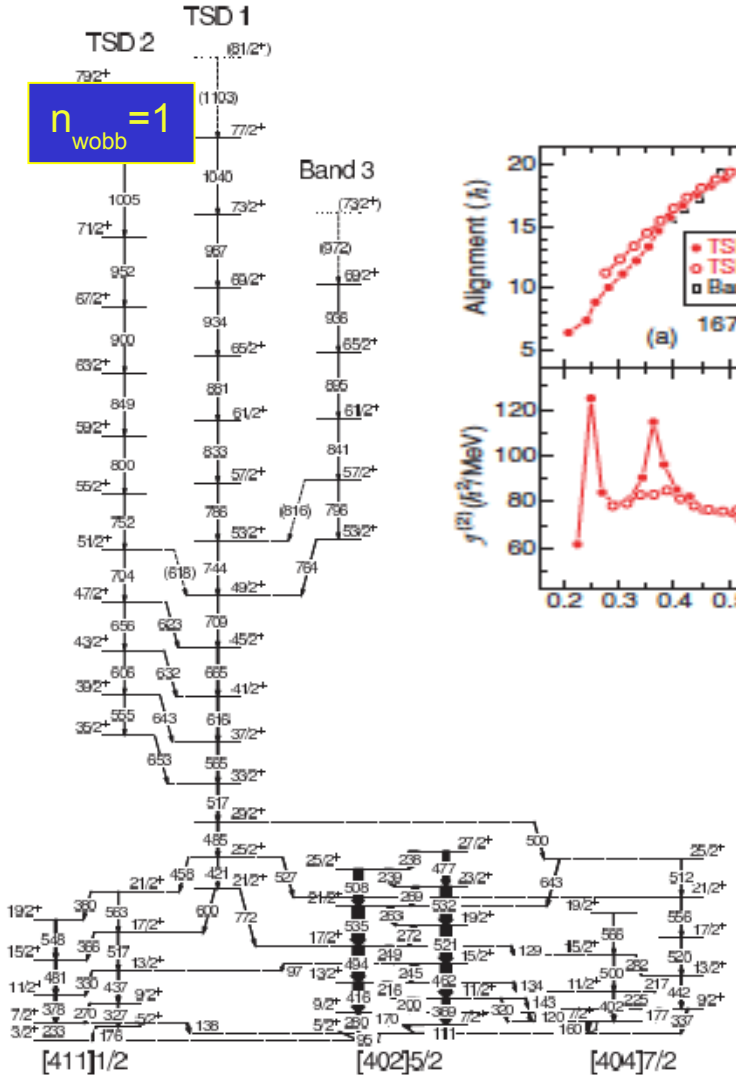

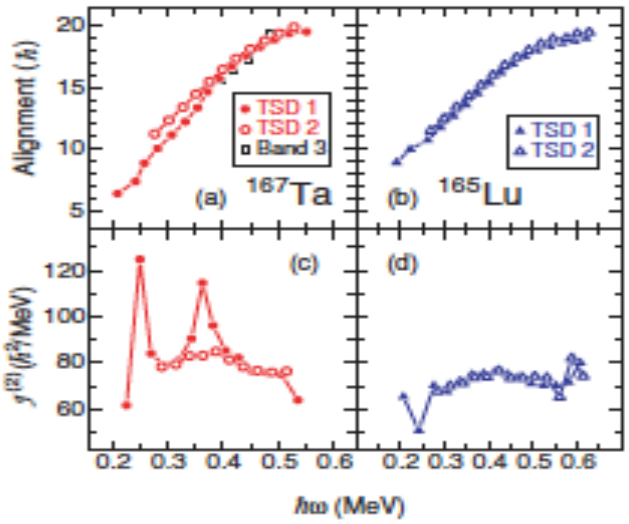

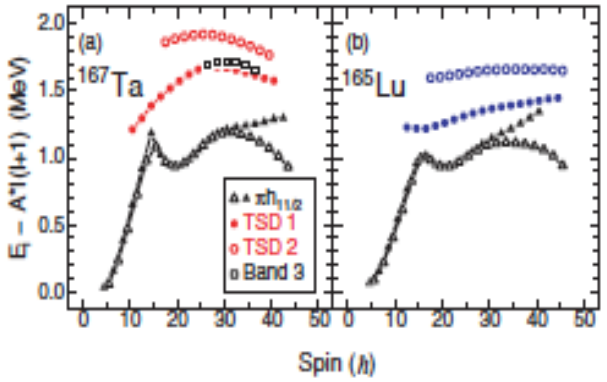

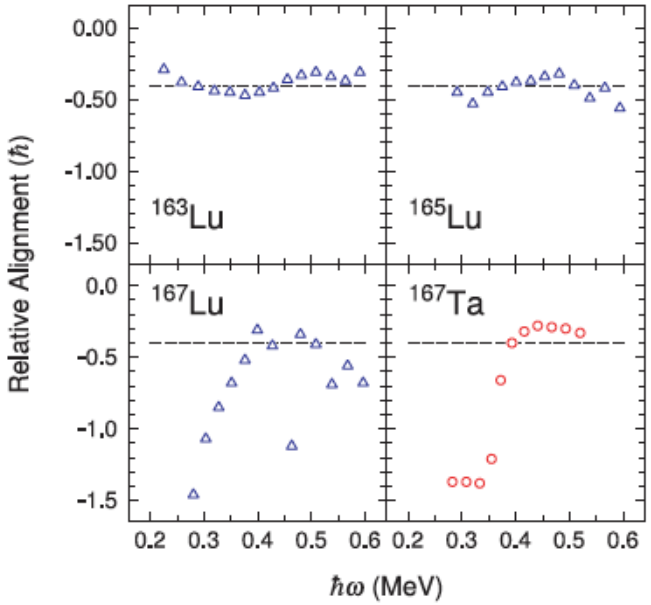

CPC(HEP & NP), 2009, **33**(Suppl. I): 145—147 Chinese Physics C Vol. 33, Suppl. I , Mar., 2009

Search for chiral bands in $A \sim 110$ neutron-rich nuclei *

ZHU Sheng-Jiang(朱胜江)[1;1)] J. H. Hamilton[2] A. V. Ramayya[2] J. K. Hwang[2] J. O. Rasmussen[3]
Y. X. Luo[2,3] K. Li[2] WANG Jian-Guo(王建国)[1] CHE Xing-Lai(车兴来)[1] DING Huai-Bo(丁怀博)[1]
S. Frauendorf[4] V. Dimitrov[4] XU Qiang(徐强)[1] GU Long(顾龙)[1] YANG Yun-Yi(杨韵颐)[1]

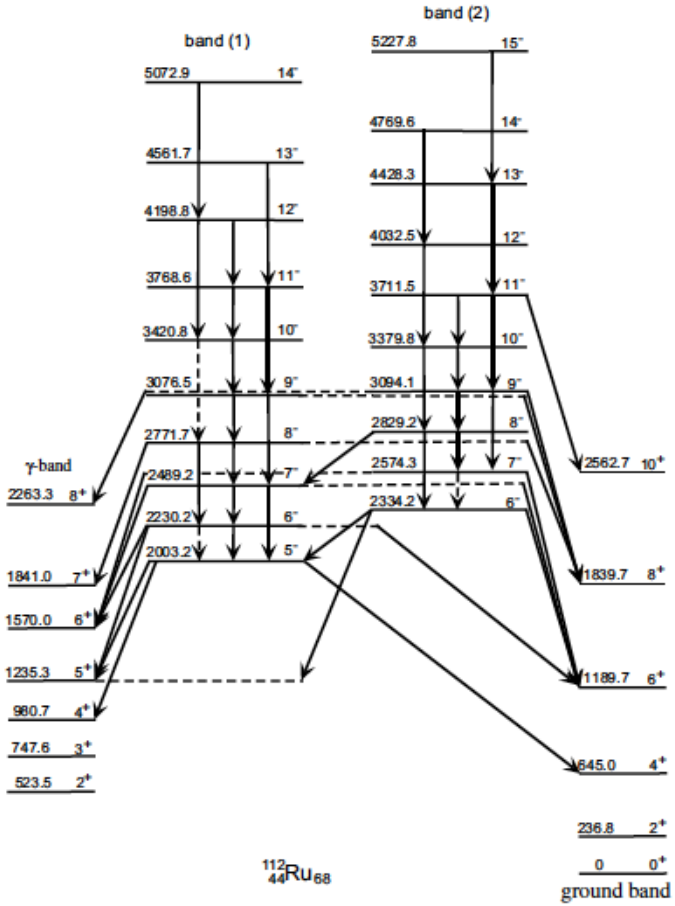

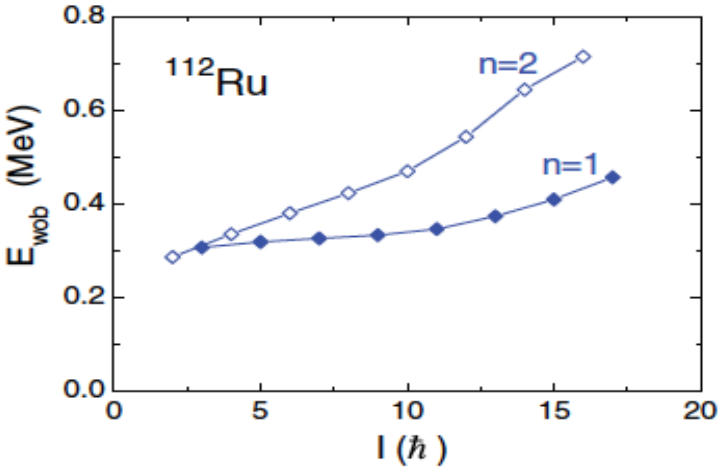

Frauendorf and Dönau, PRC 89 (2014)

Wobbling frequency

Wobbling frequency is experimentally defined by:

$$E_{wobb} = E(I, n_T=1) - \tfrac{1}{2}[E(I+1, n_T=0) + E(I-1, n_T=0)]$$

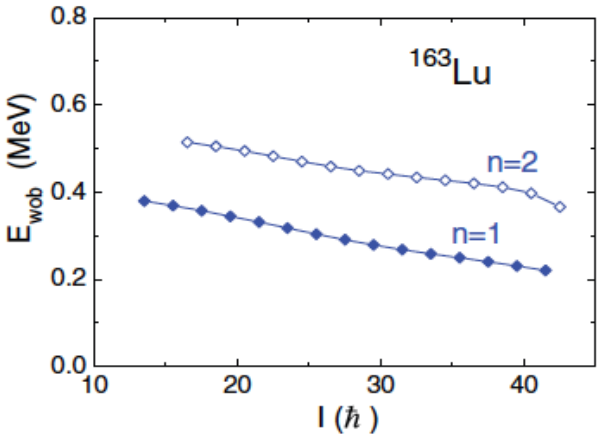

ω_{TAC} **decreases with J =>** **transransverse wobbler**

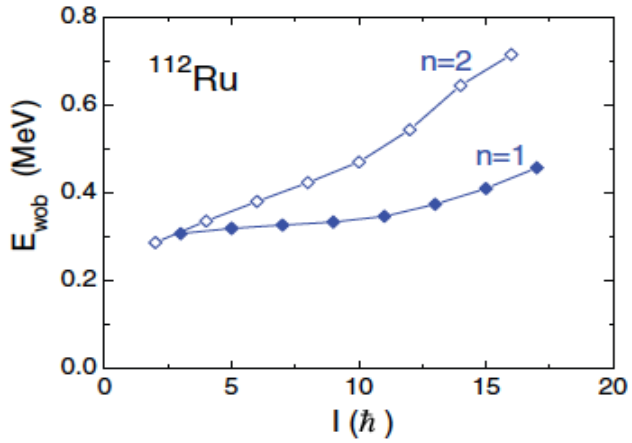

ω_{TAC} **increases with J =>** **simple wobbler**

Frauendorf and Dönau, PRC 89 (2014)

Wobbling mode

$$E(I, n_{\mathrm{wobb}}) = \frac{I(I+1)}{2\mathcal{J}_x} + \hbar\omega_{\mathrm{wobb}}\left(n_{\mathrm{wobb}} + \frac{1}{2}\right)$$

$$\hbar\omega_{wobb} = \frac{\hbar^2 J}{\mathcal{J}_3}\sqrt{\frac{(\mathcal{J}_3 - \mathcal{J}_1)(\mathcal{J}_3 - \mathcal{J}_2)}{\mathcal{J}_1\mathcal{J}_2}} \longrightarrow$$ **Simple wobbler (even-even)**

$$\hbar\omega_{wobb} = \frac{\hbar^2 j}{\mathcal{J}_3}\sqrt{\left[1 + \frac{J}{j}\left(\frac{\mathcal{J}_3}{\mathcal{J}_1} - 1\right)\right]\left[1 + \frac{J}{j}\left(\frac{\mathcal{J}_3}{\mathcal{J}_2} - 1\right)\right]} \longrightarrow$$ **Longitudinal wobbler**
Transverse wobbler

Longitudinal wobbling	$\mathcal{J}_3 > \mathcal{J}_1, \mathcal{J}_2$	ω_{TAC} **increases with J**
Transverse wobbling	$\mathcal{J}_3 > \mathcal{J}_1$ and $\mathcal{J}_3 < \mathcal{J}_2$	ω_{TAC} **decreases with J**

Fitted QTR MoI for ^{135}Pr	$\mathcal{J}_m, \mathcal{J}_s, \mathcal{J}_l = 7.4,\ 5.6,\ 1.8\hbar^2/\mathrm{MeV}$	$\mathcal{J}_m/\mathcal{J}_s/\mathcal{J}_l = 1/0.75/0.24$
TAC MoI for ^{135}Pr	$\mathcal{J}_m, \mathcal{J}_s, \mathcal{J}_l = 19,\ 8,\ 3\ \hbar^2/\mathrm{MeV}$	$\mathcal{J}_m/\mathcal{J}_s/\mathcal{J}_l = 1/0.42/0.16$
RPA MoI for ^{138}Nd	$\mathcal{J}_x, \mathcal{J}_y, \mathcal{J}_z = 35, 20, 8\ \hbar^2/MeV$	$\mathcal{J}_x/\mathcal{J}_y/\mathcal{J}_z = 1/0.57/0.23$

PHYSICAL REVIEW C 89, 014322 (2014)

Transverse wobbling: A collective mode in odd-*A* triaxial nuclei

S. Frauendorf[1,*] and F. Dönau[2,†]

Longitudinal wobber

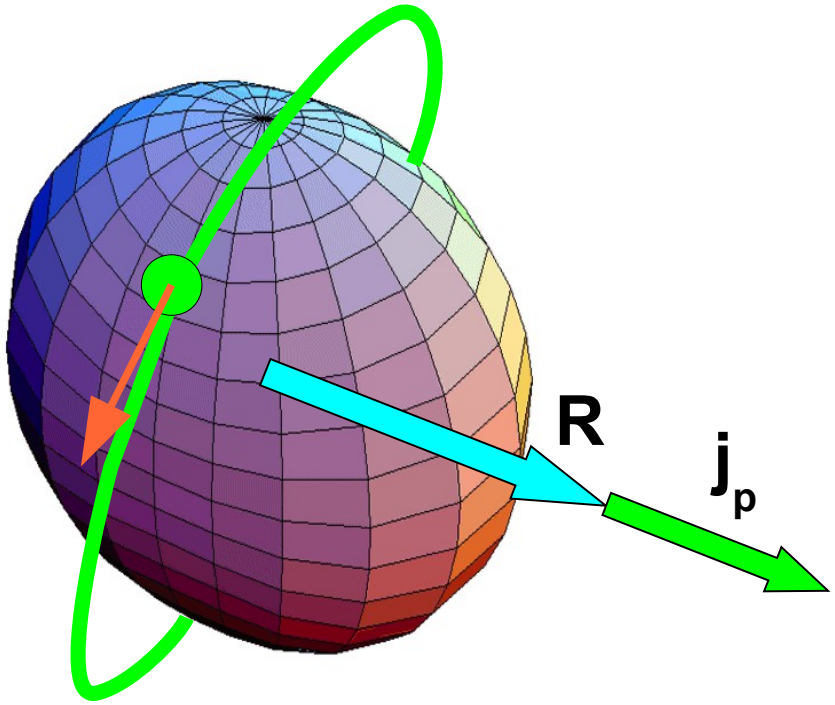

$$\mathcal{J}_3 \quad \rightarrow \quad \mathcal{J}_3^*(\omega) = \frac{\mathcal{J}_3\omega + j}{\omega} = \mathcal{J}_3 + \frac{j}{\omega}$$

Transverse wobber

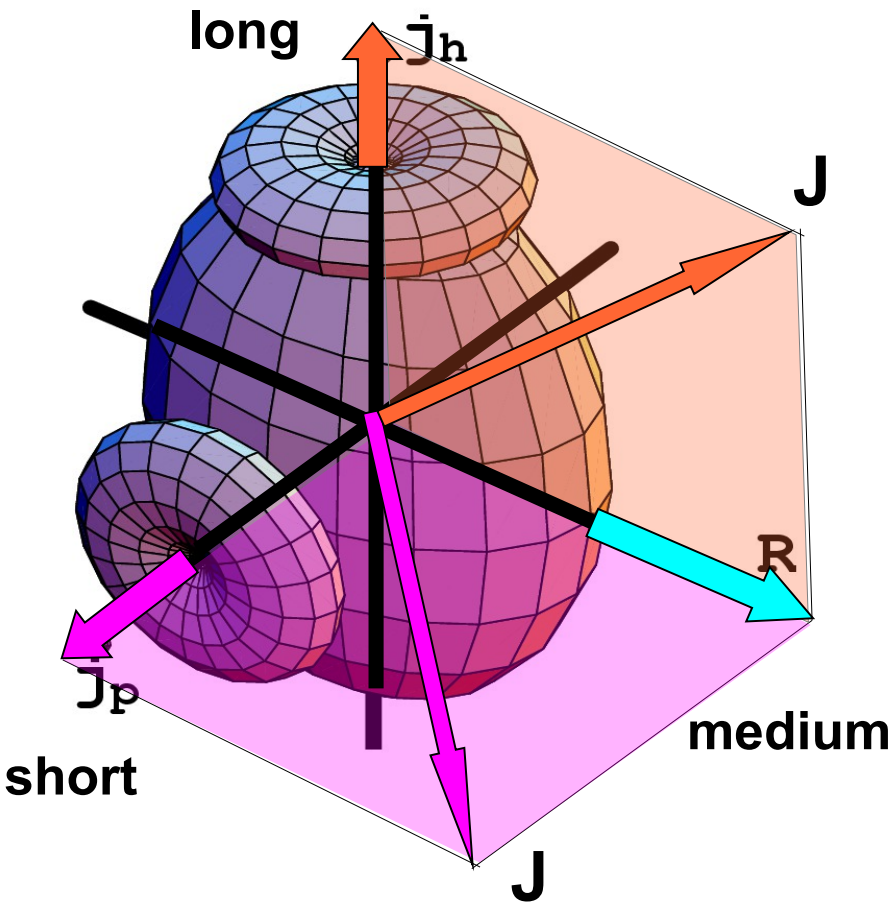

^{135}Pr

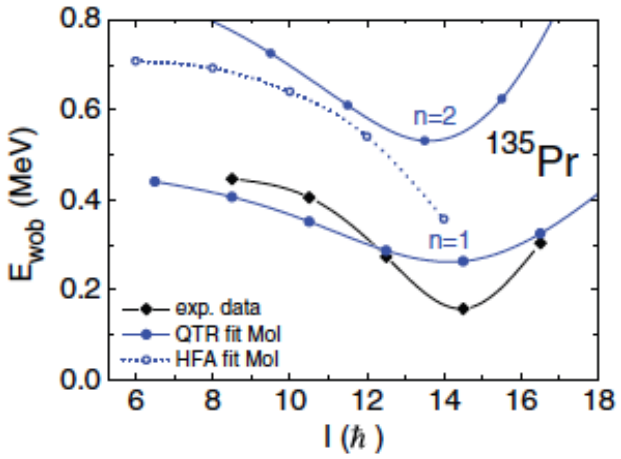

FIG. 14. (Color online) Excitation energies of the $n = 1$ and $n = 2$ wobbling bands in ^{135}Pr. Solid blue lines and full dots: QTR calculation with fitted MoI. Dotted blue lines and open dots: HFA calculation with fitted MoI. Black line and full diamonds: Experimental data.

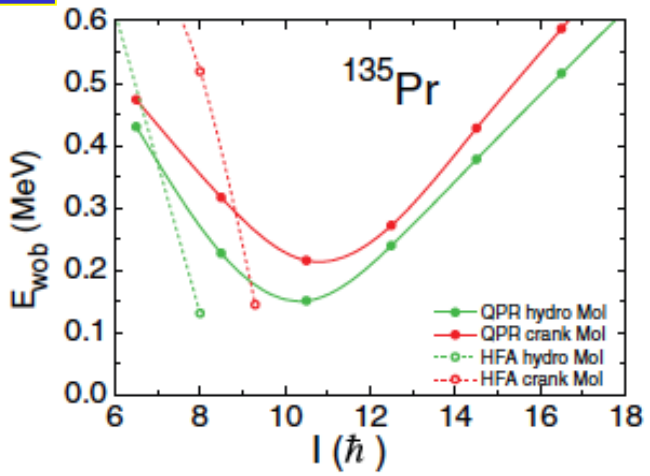

FIG. 16. (Color online) Excitation energies of the wobbling band in ^{135}Pr. Solid red lines and full dots: QTR with cranking MoI, solid green lines and full dots: QTR with hydrodynamic MoI. Dashed lines and open dots: HFA with cranking and hydrodynamic MoI, respectively.

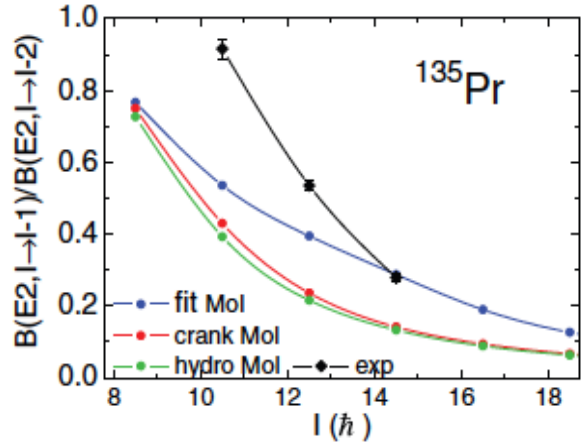

FIG. 18. (Color online) $B(E2)$ ratios of the connecting to in-band transitions $n = 1 \rightarrow n = 0$ of the wobbling band in ^{135}Pr. Solid blue line: QTR calculated with fitted moments of inertia, red (green) line: with cranking (hydrodynamic) moments of inertia. Black: Experimental data (cf. Table II).

Frauendorf and Dönau, PRC 89 (2014)

^{163}Lu

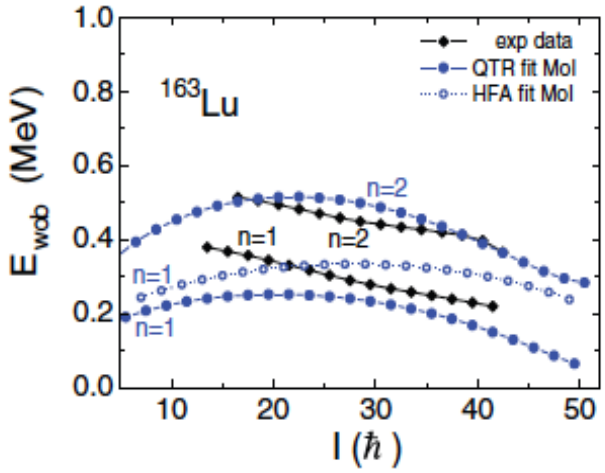

FIG. 13. (Color online) Excitation energies of the $n = 1$ and $n = 2$ wobbling bands in ^{163}Lu. Solid blue lines and full dots: QTR calculation with fitted MoI. Dotted blue line and open dots: HFA calculation for the $n = 1$ band with fitted MoI. Black lines and full diamonds: Experimental data.

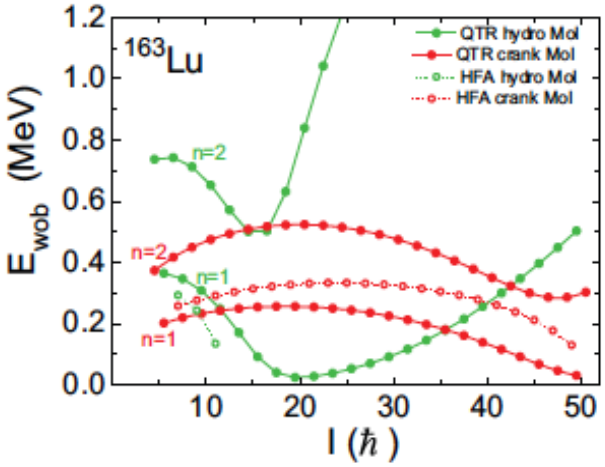

FIG. 15. (Color online) Excitation energies of the $n = 1$ and $n = 2$ wobbling bands in ^{163}Lu. Solid red lines and full dots: QTR with cranking MoI, solid green lines and full dots: QTR with hydrodynamic MoI. Dotted lines and open dots: HFA with cranking and hydrodynamic MoI, respectively.

Frauendorf and Dönau, PRC 89 (2014)

Wobbling in A=130-140 nuclei

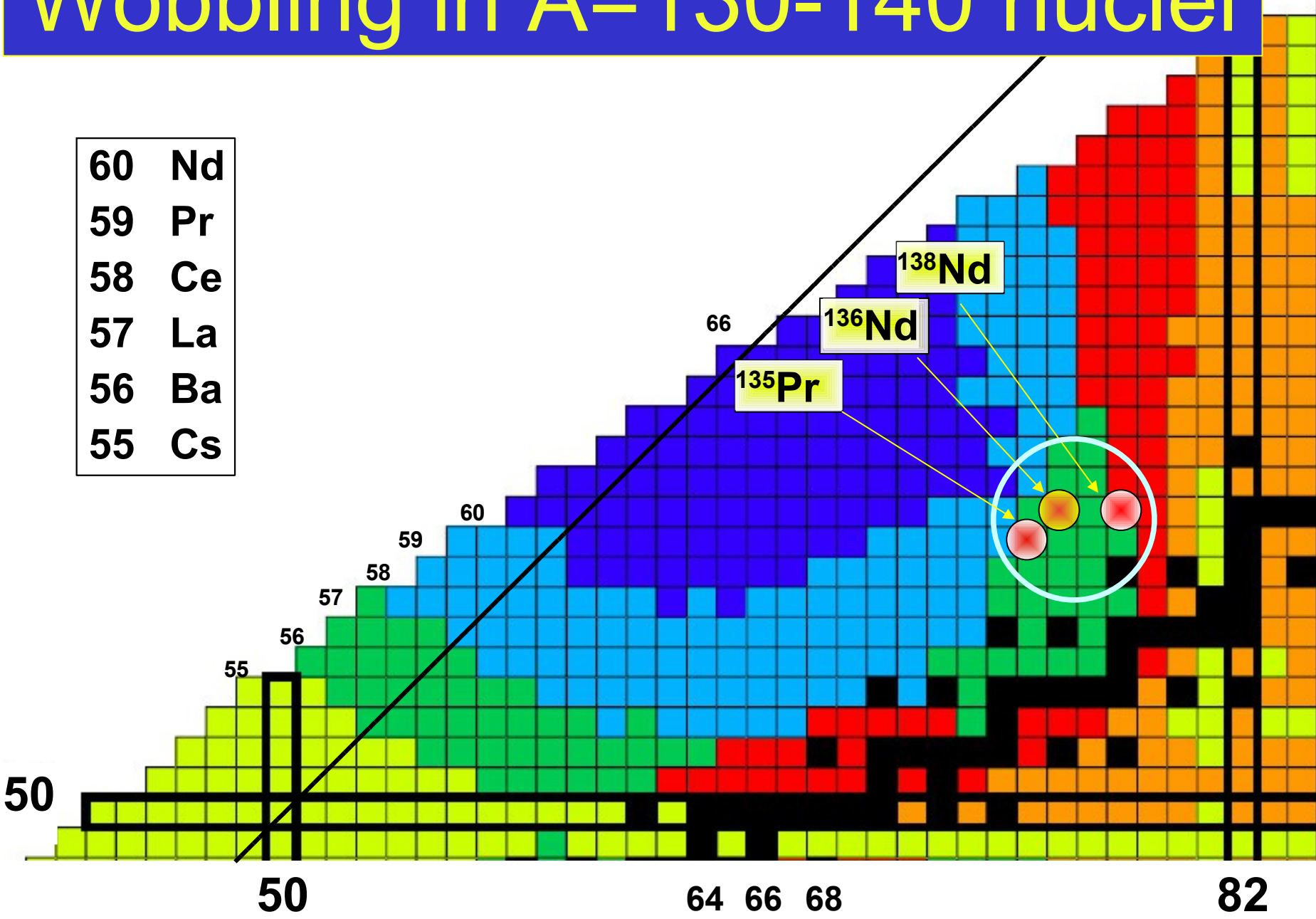

PHYSICAL REVIEW C VOLUME 34, NUMBER 2 AUGUST 1986

Spectroscopic study of the high-spin states in ^{135}Pr

T. M. Semkow, D. G. Sarantites, K. Honkanen,* V. Abenante, and L. A. Adler
Department of Chemistry, Washington University, St. Louis, Missouri 63130

^{120}Sn(^{19}F,4n)

^{135}Pr

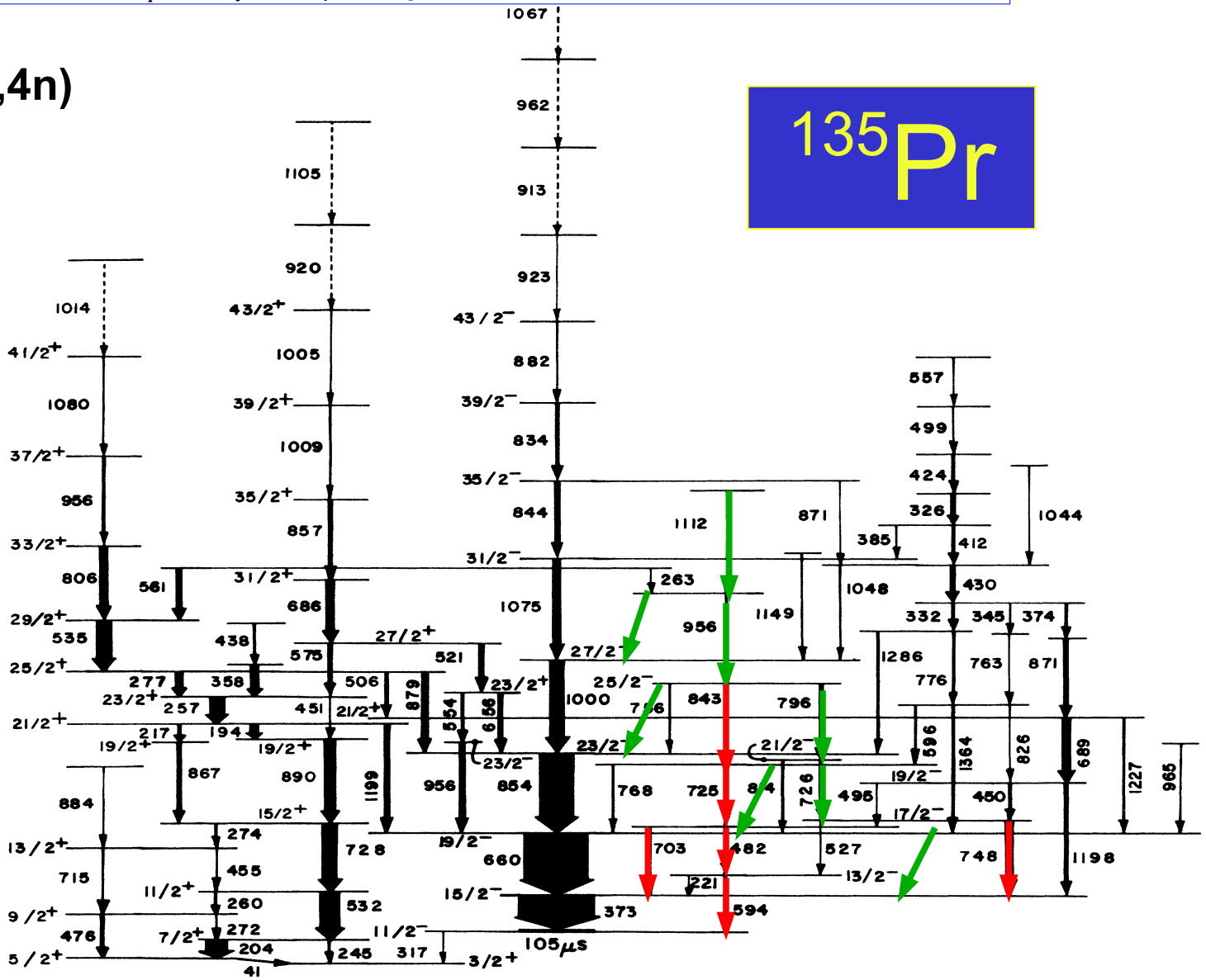

^{135}Pr

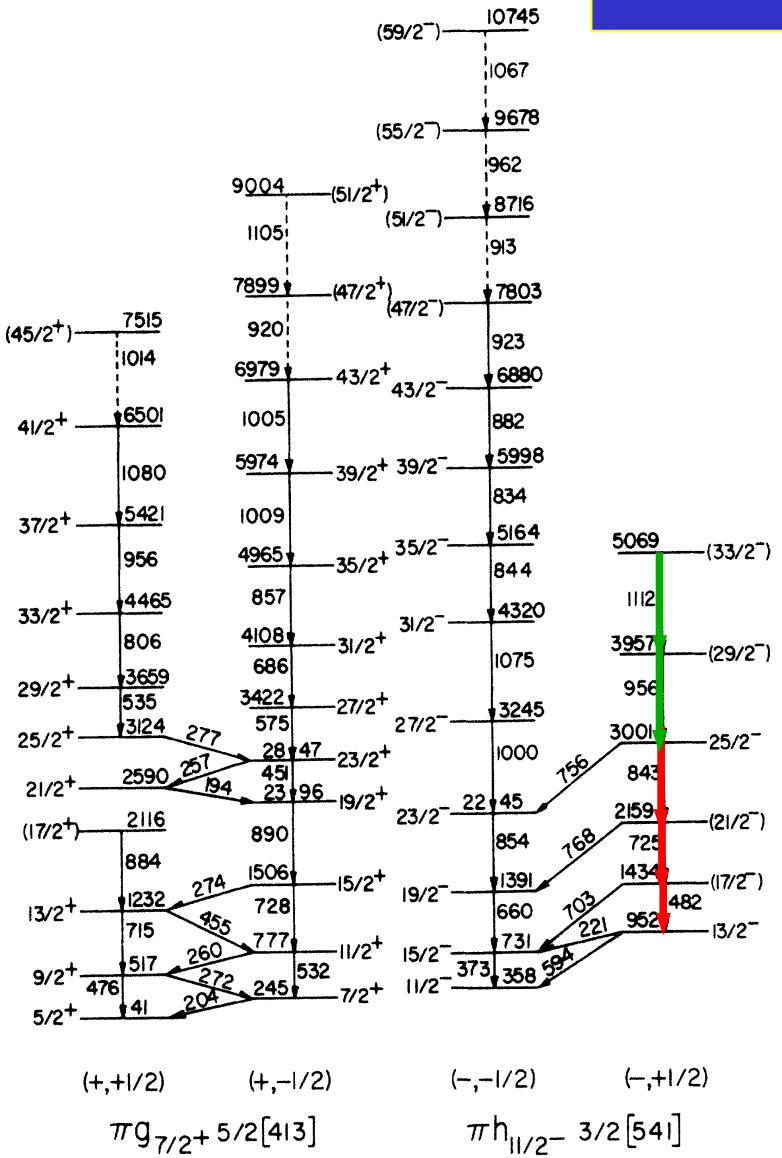

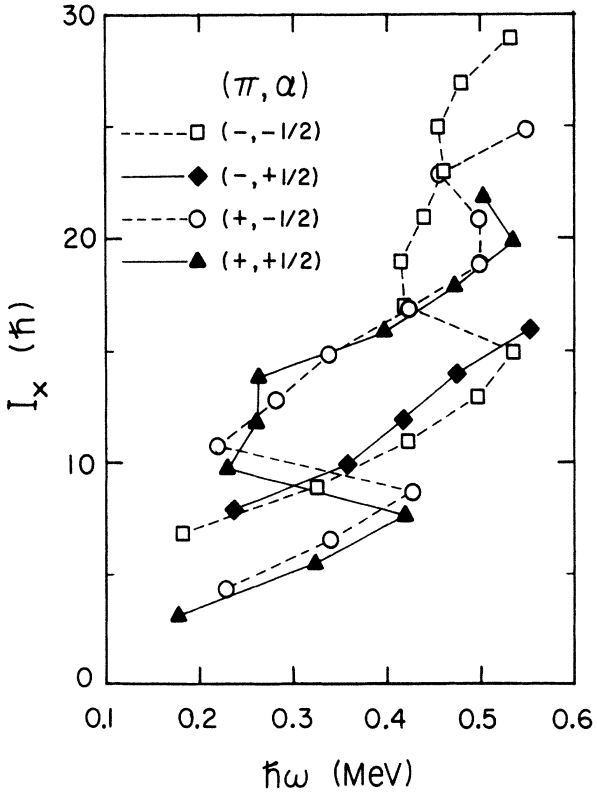

PHYSICAL REVIEW C VOLUME 58, NUMBER 6 DECEMBER 1998

Lifetime measurements in ^{135}Pr

S. Botelho,* W. A. Seale, L. G. R. Emediato, J. R. B. Oliveira, M. N. Rao, R. V. Ribas, N. H. Medina, E. W. Cybulska, M. A. Rizzutto, and F. R. Espinoza-Quiñones
Laboratório Pelletron, Departamento de Física Nuclear, Instituto de Física, Universidade de São Paulo, São Paulo, Brazil

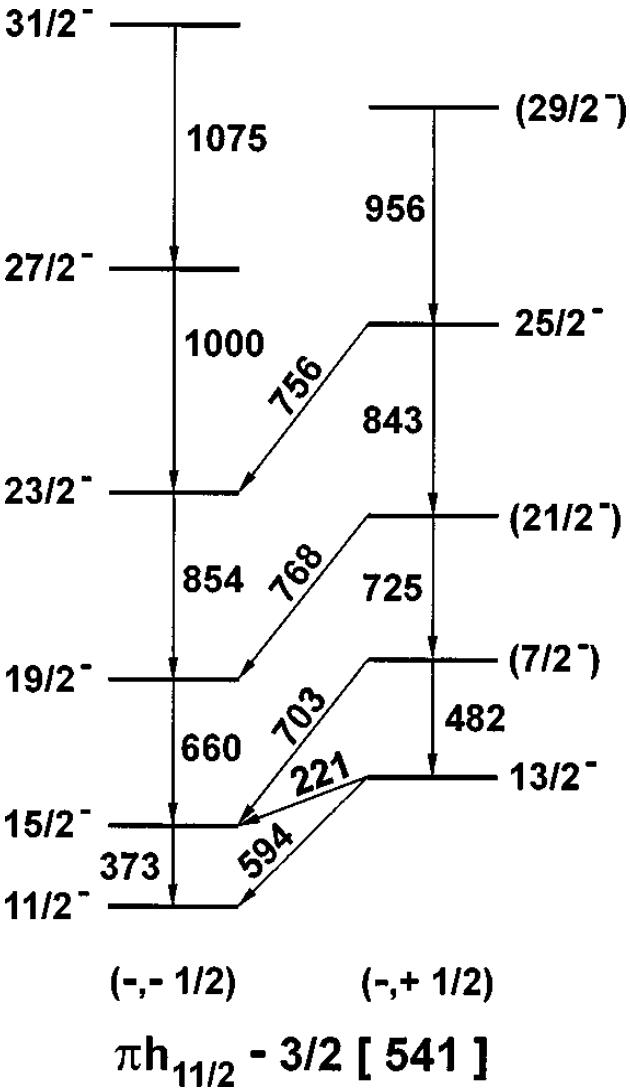

^{123}Sb(^{16}O,4n)

^{135}Pr

TABLE II. Experimental values of the quadrupole moments, and those calculated by TRS for the ^{135}Pr and ^{134}Ce nuclei.

Nucleus	J^π	Q_t^{expt} (e b)	Q_t^{TRS} (e b)
	$15/2^-$	3.2±0.1	
^{135}Pr[a]	$19/2^-$	2.4±0.3	2.2
	$23/2^-$	1.98±0.05	
	2^+	3.3±0.2	
^{134}Ce[b]	4^+	2.44±0.01	3.4
	6^+	1.60±0.08	

[a]Spins and parities from Ref. [2].
[b]From Ref. [5].

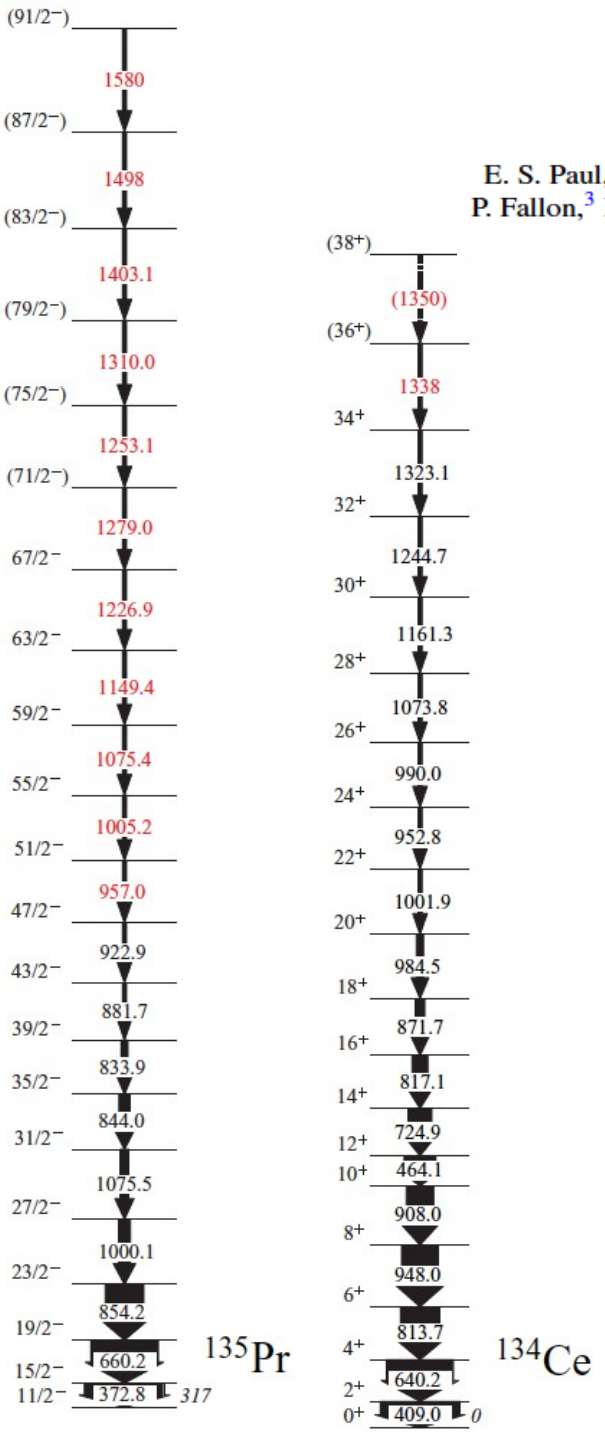

PHYSICAL REVIEW C 84, 047302 (2011)

High-spin yrast states in the γ-soft nuclei ^{135}Pr and ^{134}Ce

E. S. Paul,[1] C. Fox,[1] A. J. Boston,[1] H. J. Chantler,[1] C. J. Chiara,[2,*] R. M. Clark,[3] M. Cromaz,[3] M. Descovich,[1] P. Fallon,[3] D. B. Fossan,[2] A. A. Hecht,[4,†] T. Koike,[2,‡] I. Y. Lee,[3] A. O. Macchiavelli,[3] P. J. Nolan,[3] K. Starosta,[2,§] R. Wadsworth,[5] and I. Ragnarsson[6]

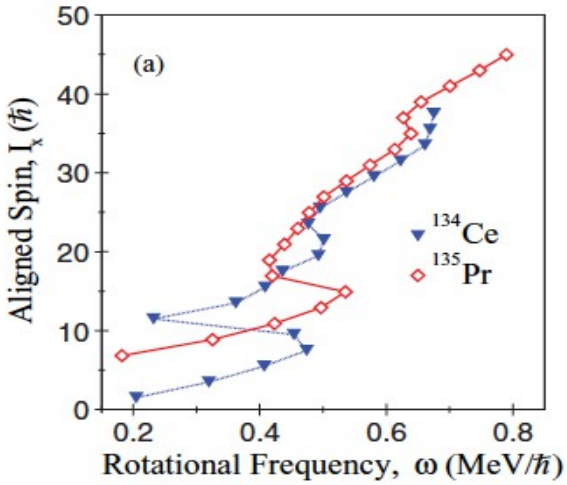

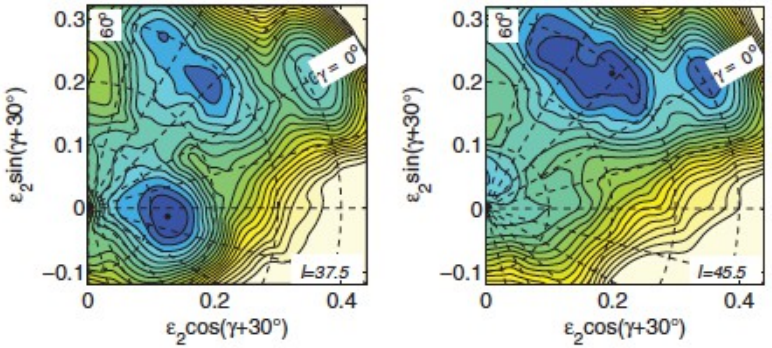

FIG. 4. (Color online) Calculated potential-energy surfaces for negative-parity configurations at spin values $I = 75/2$ and $91/2$ (signature, $\alpha = -1/2$). The contour line separation is 0.25 MeV.

PRL 114, 082501 (2015) PHYSICAL REVIEW LETTERS week ending 27 FEBRUARY 2015

Transverse Wobbling in ^{135}Pr

J. T. Matta, U. Garg, W. Li, S. Frauendorf, A. D. Ayangeakaa,† D. Patel, and K. W. Schlax
Physics Department, University of Notre Dame, Notre Dame, Indiana 46556, USA

^{135}Pr

^{123}Sb(^{16}O,4n)

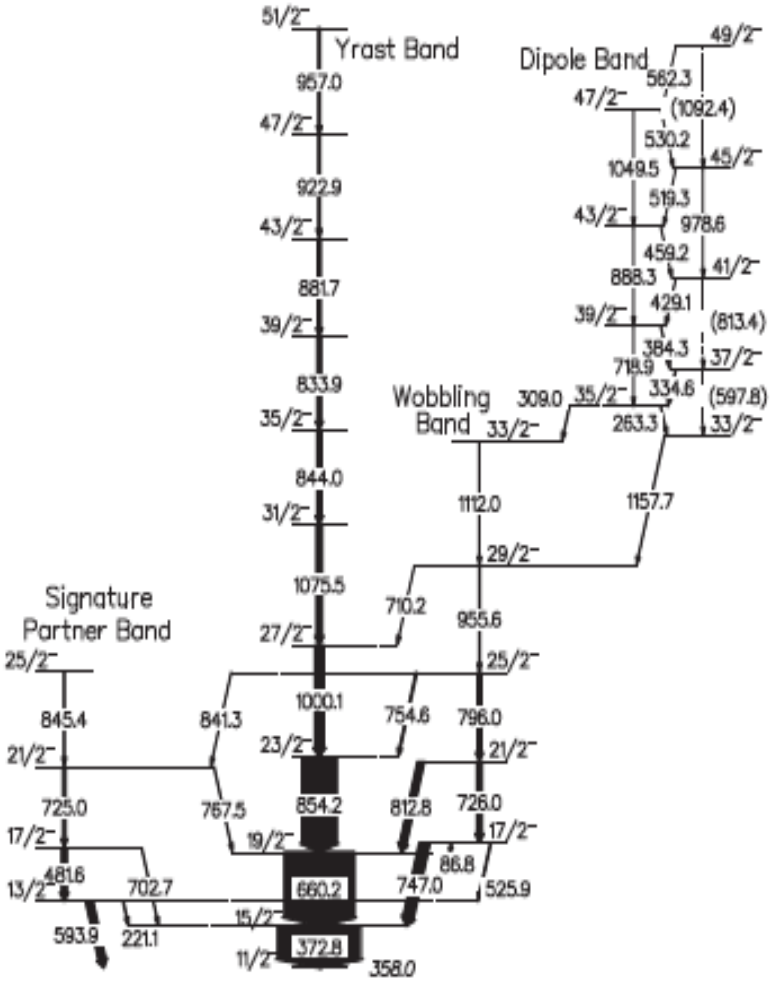

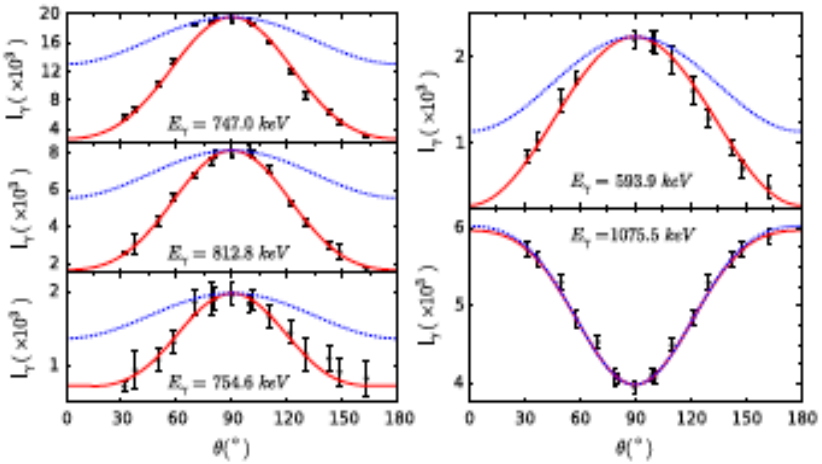

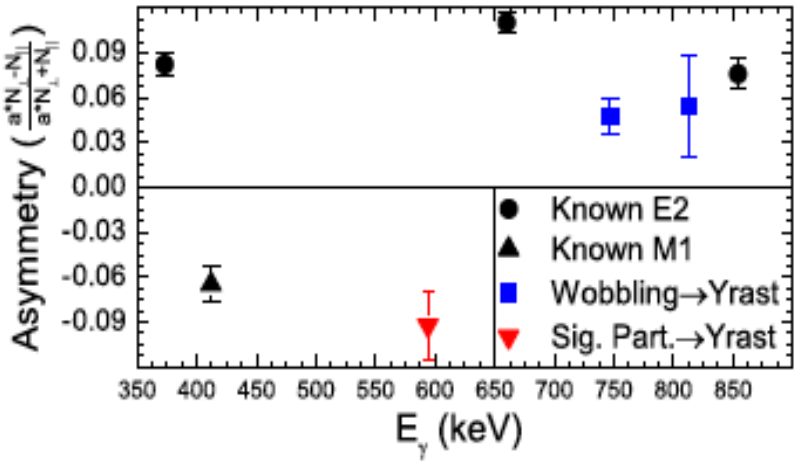

^{135}Pr

TABLE I. The mixing ratios, δ, E2 fractions, and the experimental and theoretical transition probability ratios for transitions from the $n_\omega = 1$ to $n_\omega = 0$ wobbling bands in γ. The in-band transitions were assumed to be of pure E2 character in calculations of the probability ratios. The mixing ratio of the $\frac{25^-}{2} \rightarrow \frac{23^-}{2}$ transition has been taken as a lower limit when deriving the probability ratios for the $\frac{29^-}{2} \rightarrow \frac{27^-}{2}$ transition. Shown at the bottom is the measured mixing ratio for the lowest Signature partner to Yrast transition.

Initial I^π	Final I^π	E_γ (keV)	δ	Asymmetry	E2 Fraction (%)	$\frac{B(M1_{out})}{B(E2_{in})}\left(\frac{\mu_N^2}{e^2b^2}\right)$ Experiment	QTR	$\frac{B(E2_{out})}{B(E2_{in})}$ Experiment	QTR
$\frac{17^-}{2}$	$\frac{15^-}{2}$	747.0	-1.24 ± 0.13	0.047 ± 0.012	60.6 ± 5.1	...	0.213	...	0.908
$\frac{21^-}{2}$	$\frac{19^-}{2}$	812.8	-1.54 ± 0.09	0.054 ± 0.034	70.3 ± 2.4	0.164 ± 0.014	0.107	0.843 ± 0.032	0.488
$\frac{25^-}{2}$	$\frac{23^-}{2}$	754.6	-2.38 ± 0.37	...	85.0 ± 4.0	0.035 ± 0.009	0.070	0.500 ± 0.025	0.290
$\frac{29^-}{2}$	$\frac{27^-}{2}$	710.2	...	...	...	$\leq 0.016 \pm 0.004$	0.056	$\geq 0.261 \pm 0.014$	0.191
$\frac{13^-}{2}$	$\frac{11^-}{2}$	593.9	-0.16 ± 0.04	-0.092 ± 0.023	2.5 ± 1.2	...	...	...	...

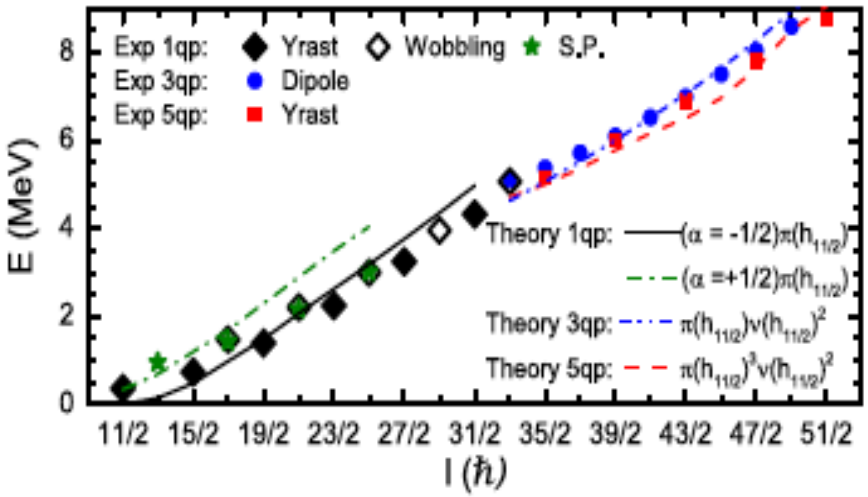

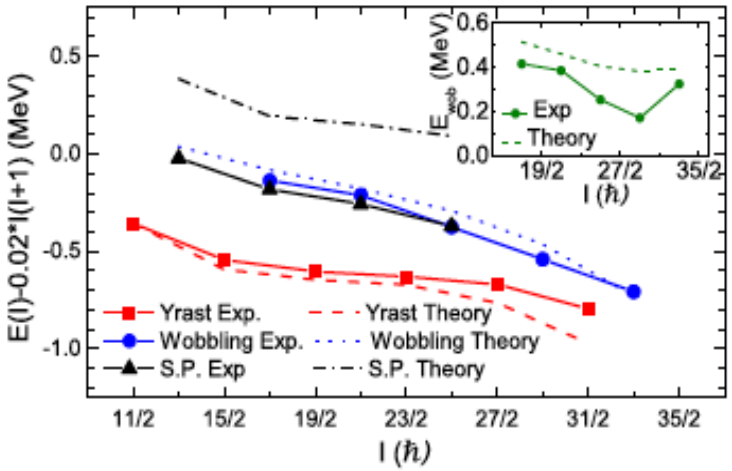

CNS calculations for ^{138}Nd

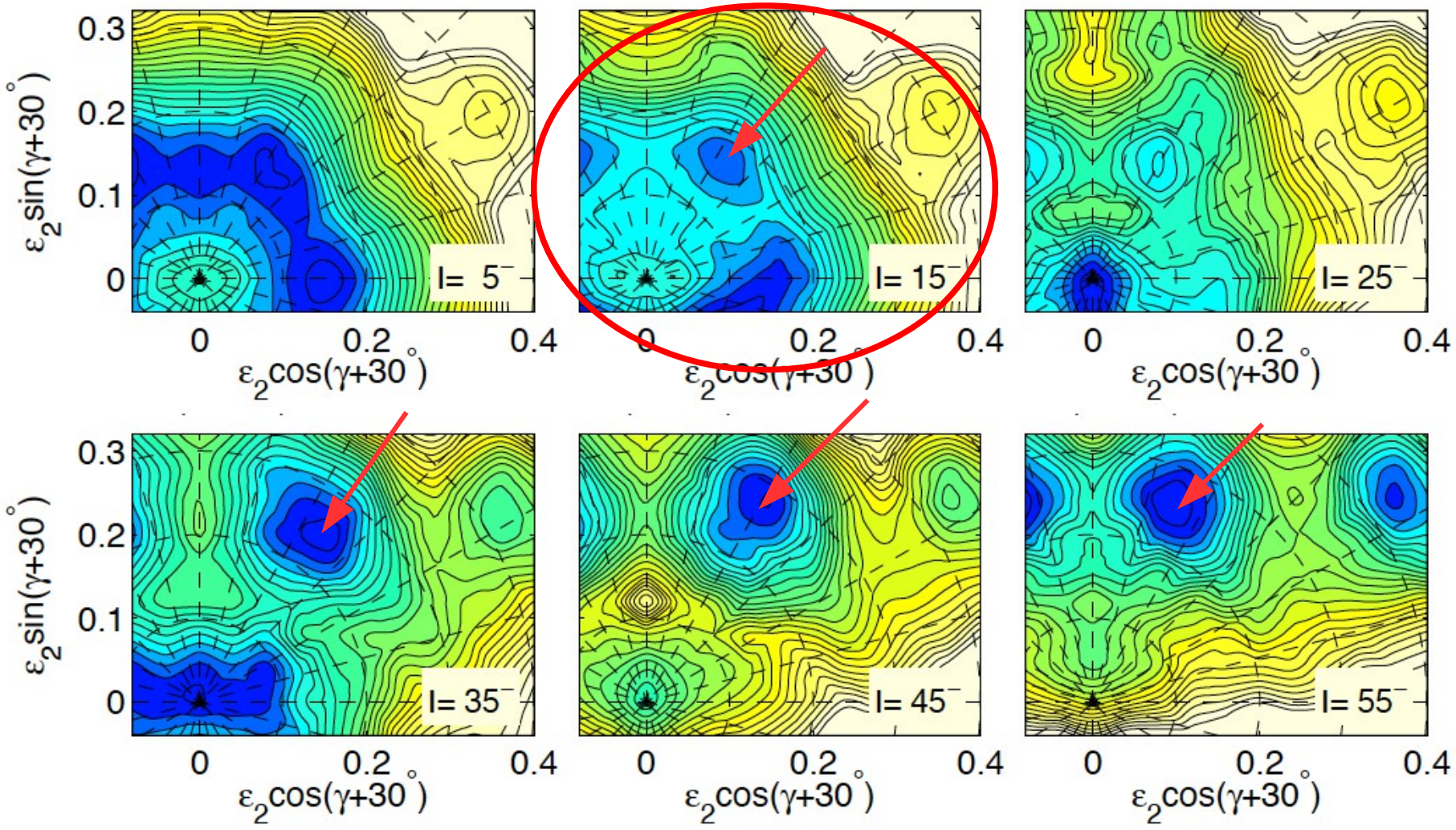

FIG. 3: The PES of the configuration $\pi_p = -, \alpha_p = 1, \pi_n = +, \alpha_n = 0$ for ^{138}Nd.

I. Ragnarsson

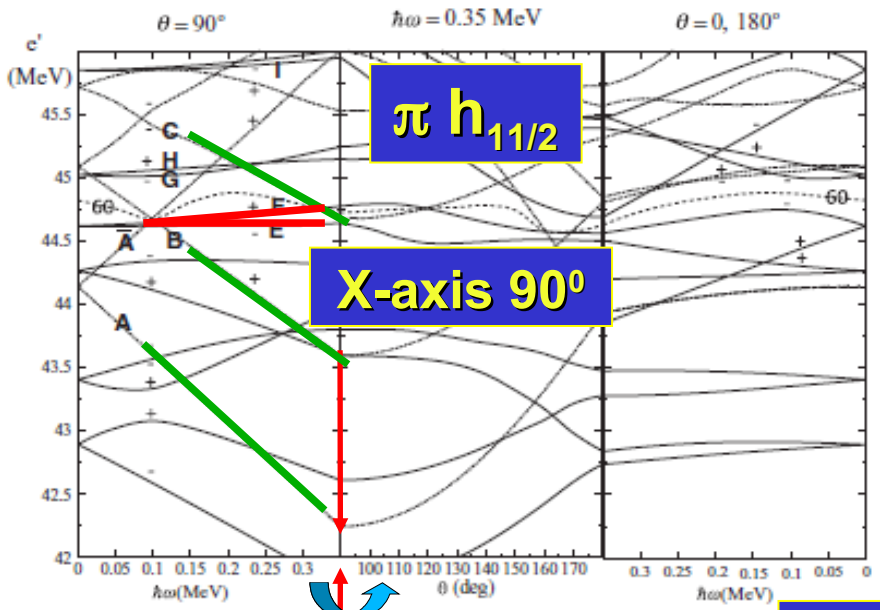

π $h_{11/2}$

X-axis 90⁰

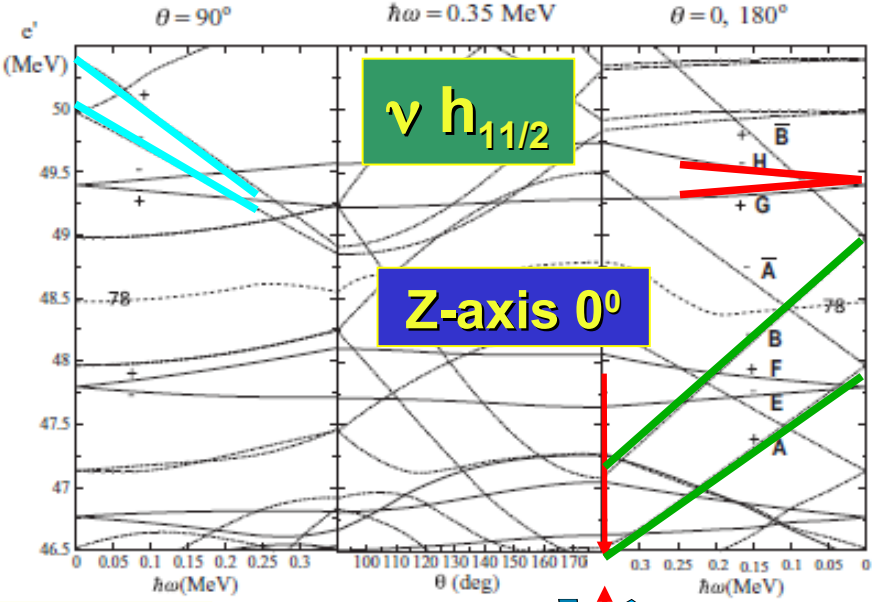

ν $h_{11/2}$

Z-axis 0⁰

E2 bands

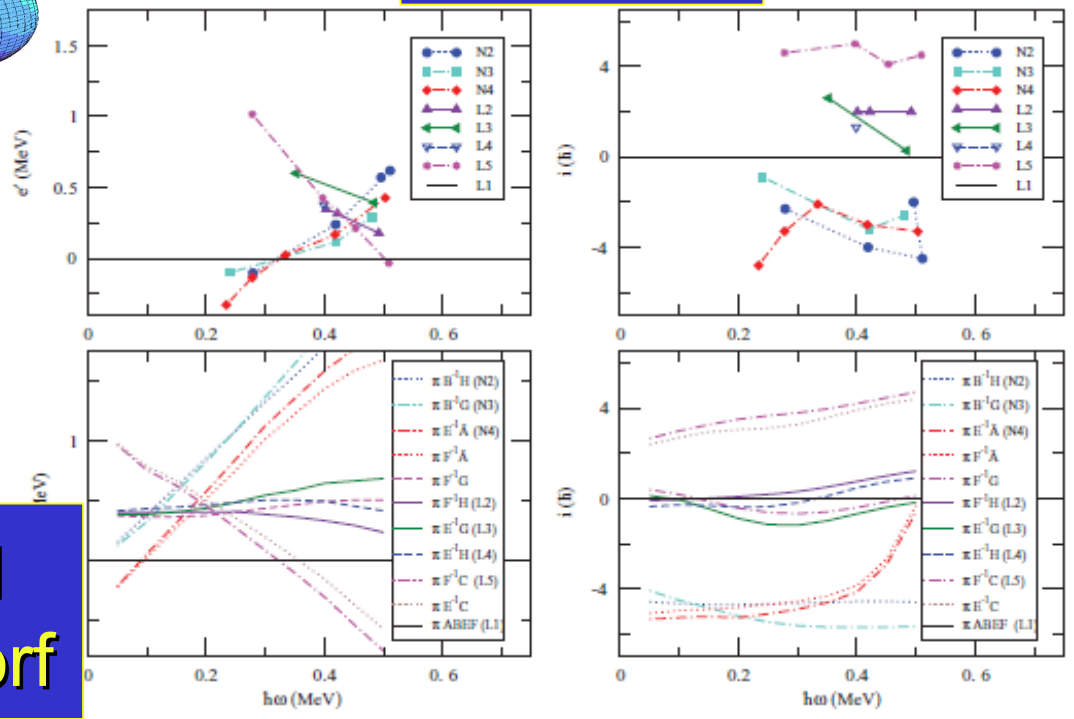

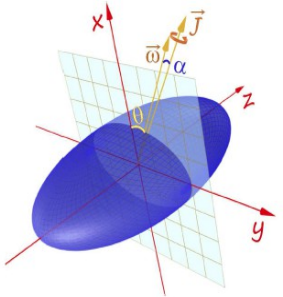

TAC, CSM
S. Frauendorf

^{138}Nd

15 high-spin bands

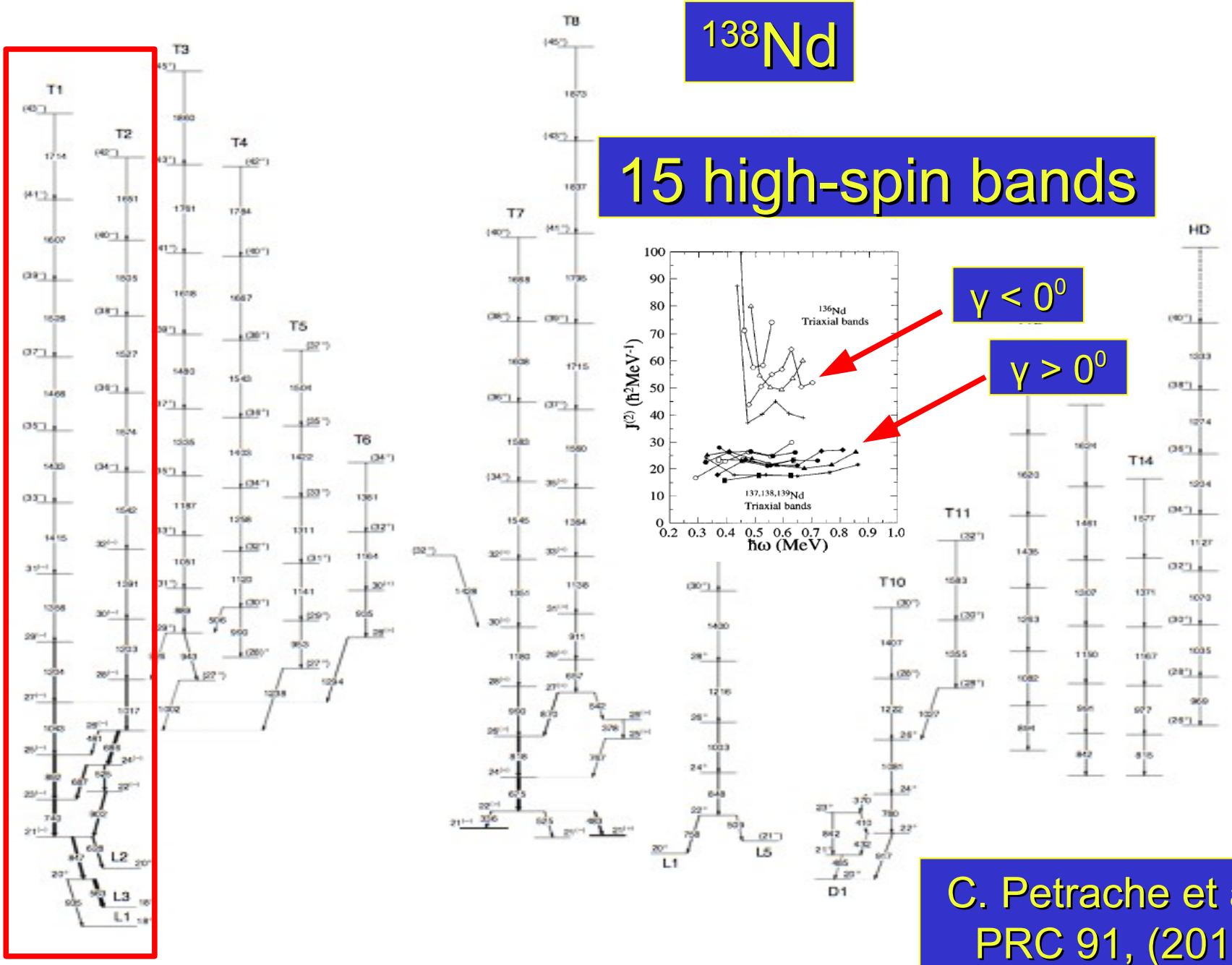

C. Petrache et al., PRC 91, (2015)

Switch of rotation from short to intermediate axis at high spin in ^{138}Nd

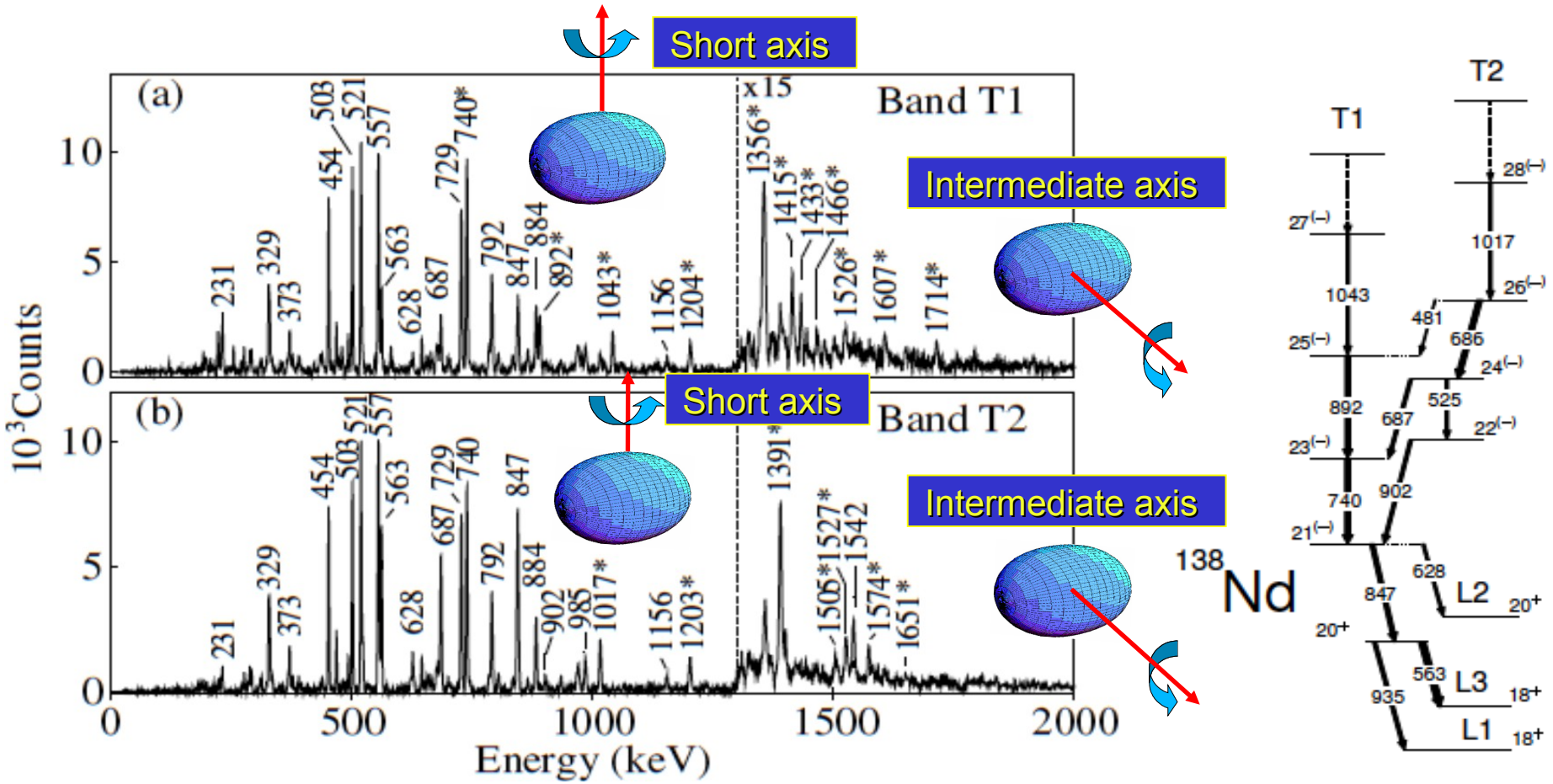

C. Petrache et al., PRC(R) 2013

Band L7 of ^{138}Nd – transverse wobbling

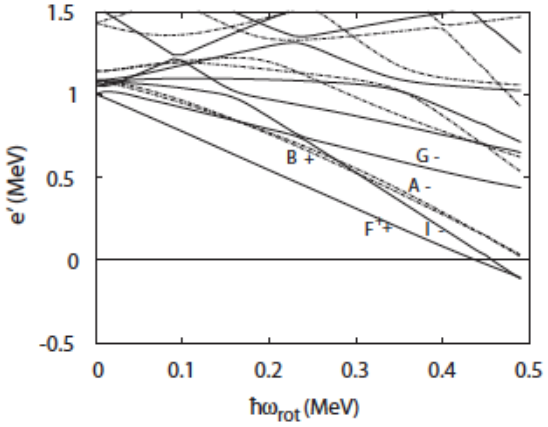

Here and further in this paragraph the proton configurations are taken relative to the g vacuum. Figure 16 indicates that the lowest even-spin excitation is $\pi F^{\dagger} I \otimes \nu 10$. As seen in Fig. 17, it can be assigned to the observed band L8. In contrast, the observed odd-spin band L7 cannot be associated with any calculated two-quasiparticle excitation. Figure 17(b) shows that the lowest odd-spin configuration $\pi G I \otimes \nu 10$ is calculated at a much higher excitation energy than the lowest even-spin $\pi F^{\dagger} I \otimes \nu 10$ configuration. This is in disagreement with the experimental bands L7 and L8 shown in Fig. 17(a), the Routhians of which almost continue each other.

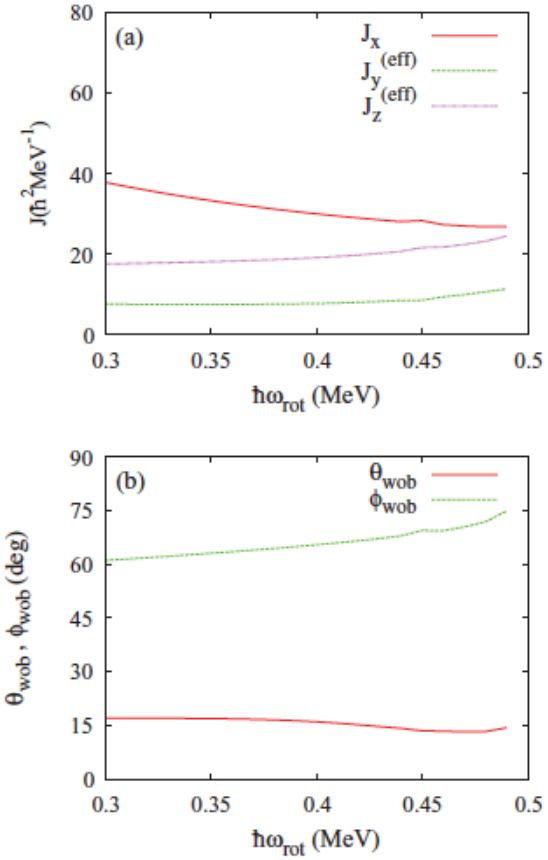

Figure 18 shows almost all solutions located lower than 1 MeV. We will focus on the two lowest solutions among them. The character of the solutions must be judged as follows: First of all, the collective solutions are located at low energies, being well separated from other noncollective ones in ideal cases. Second, their wave functions are distributed over many two-quasiparticle states in a way which enhances certain transition amplitudes, such as in the case of the γ vibration mode, in which the $K = 2$ transition amplitudes are dominant. In the case of the present lowest solution, the $K = 1$ and 2 transition amplitudes are strong and fully mixed with a definite phase relation, which would lead to a characteristic staggering of $B(E2)$ [39]. Further information that signals the wobbling character of the solution is obtained from the calculated three moments of inertia [cf. Fig. 19(a)] and the calculated wobbling angles [38] [cf. Fig. 19(b)]. In particular, the calculated moments of inertia can be understood by assuming an irrotational-like γ dependence ($\mathcal{J}_x < \mathcal{J}_z$) superimposed by the contribution to $\mathcal{J}_x$ from the aligned νh^2 pair. This makes $\mathcal{J}_x > \mathcal{J}_z$, as in the celebrated case of ^{163}Lu, where a $\pi i_{13/2}$ orbital makes $\mathcal{J}_x > \mathcal{J}_y$ [6,39]. Thus we propose to interpret the observed band L7 as a wobbling mode, although its vacuum is not a well-deformed state.

^{138}Nd

wobbling

chiral

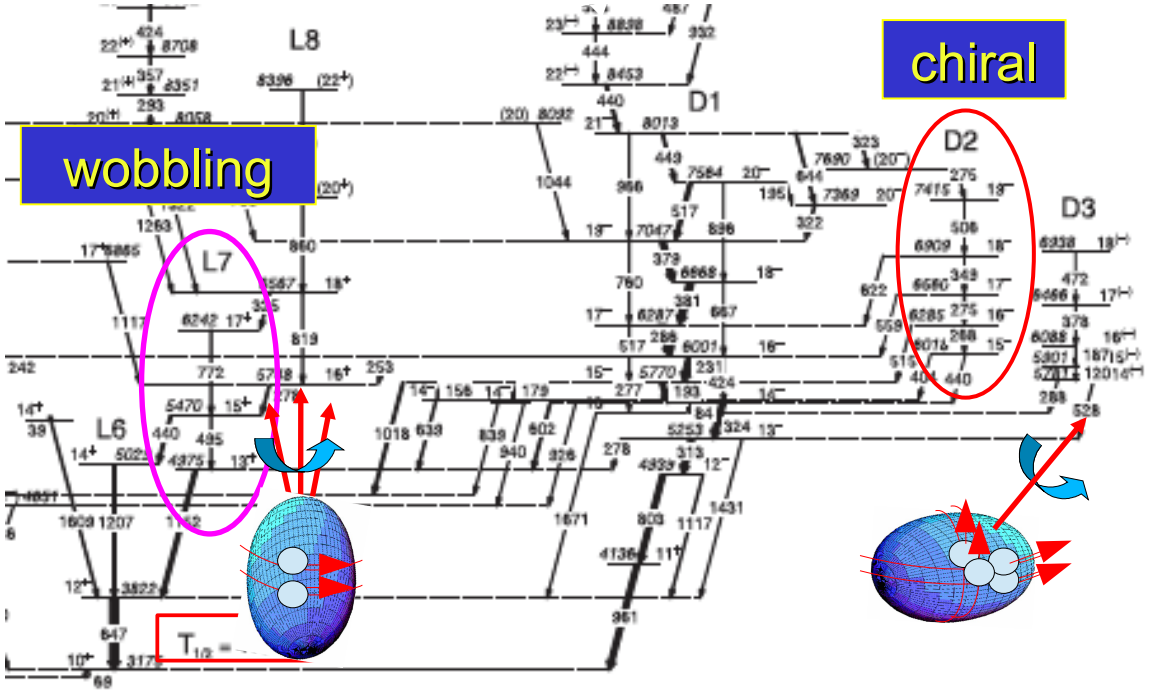

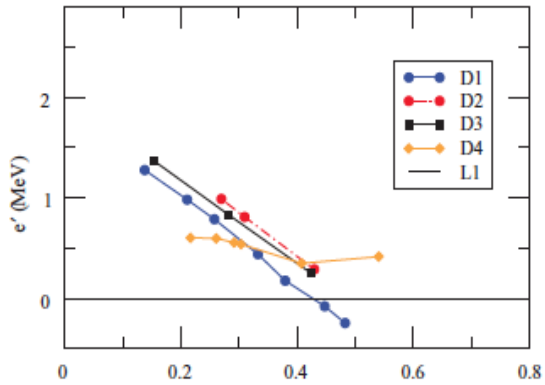

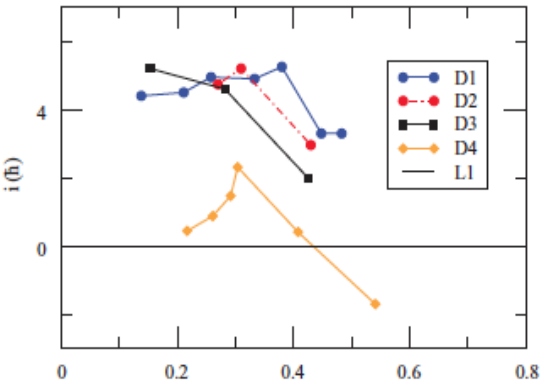

C. Petrache et al., PR C86, 044321 (2012)

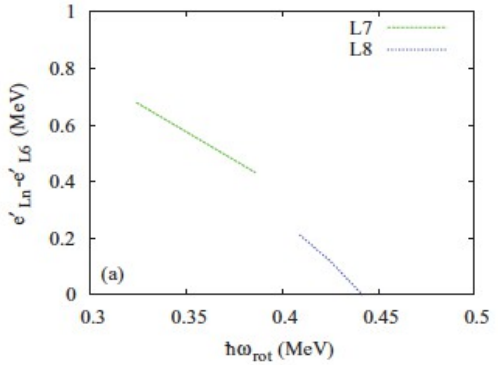

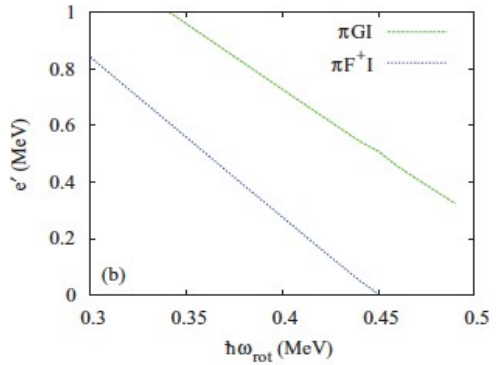

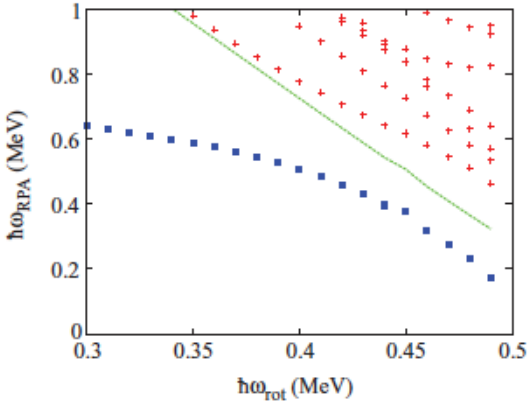

$$\omega^2 = \omega_{\rm rot}^2 \frac{[\mathcal{J}_x - \mathcal{J}_y^{(\rm eff)}(\omega)][\mathcal{J}_x - \mathcal{J}_z^{(\rm eff)}(\omega)]}{\mathcal{J}_y^{(\rm eff)}(\omega)\mathcal{J}_z^{(\rm eff)}(\omega)}$$

M. Matsuzaki

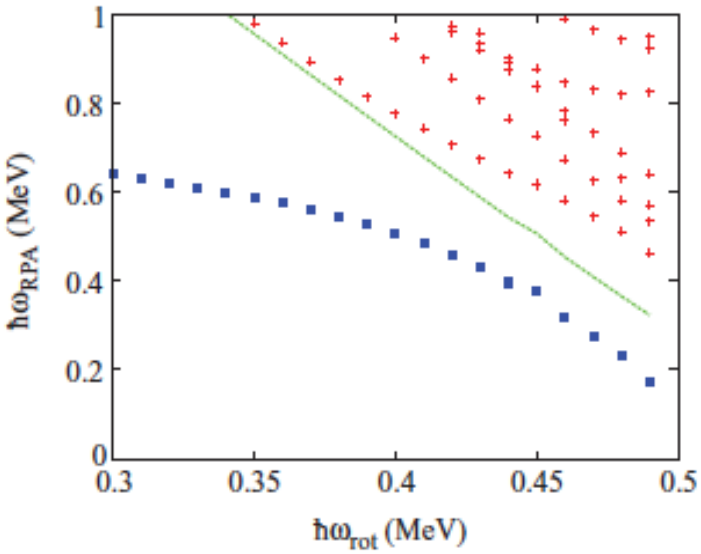

In the frequency range in which the lowest solution is collective, the second lowest solution is almost purely the two-quasiparticle state πGI, whose Routhian is shown by the green dotted curve. As ω increases, the πGI component in the RPA wave function moves gradually from the second to the lowest solution, and eventually the lowest solution becomes unstable.

In general, the instability of a collective mode leads to a "phase transition" of the mean field to a lower symmetry. In the case of the wobbling mode around a principal axis, the corresponding new mean field is a tilted-axis rotating state [38]. Rotation about a tilted axis is expected to be observed as a $\Delta I = 1$ dipole band [23], as will be discussed in the next section. In the present case the instability is triggered by the steep lowering of the lowest πGI two-quasiparticle state. The tilted-axis state appearing after this instability is expected to contain νh^2 and one or two $\pi(dg)$. The calculated frequency of the instability, $\hbar\omega_{\rm rot} \sim 0.5$ MeV, is larger than the frequency of the highest transition observed in band L7, $\hbar\omega_{\rm rot} = 0.386$ MeV.

Interpreting band L7 as the one-phonon excitation, one is tempted to assign L8 to the two-phonon excitation, because it has even spin. However Fig. 17(a) indicates that the frequency ranges of L7 and L8 are displaced from each other and that L8 is lower than L7 when the bands are extrapolated to a common frequency.

The existence of stable triaxial shape at high spins in Lanthanides with N < 82 is supported by more than 70 bands

Nucleus	Number of triaxial bands		
		Quadrupole bands	**Dipole bands**
^{138}Nd	35	27	8
^{139}Nd	8	3	5
^{140}Nd	23	12	11
^{141}Nd	7	4	3

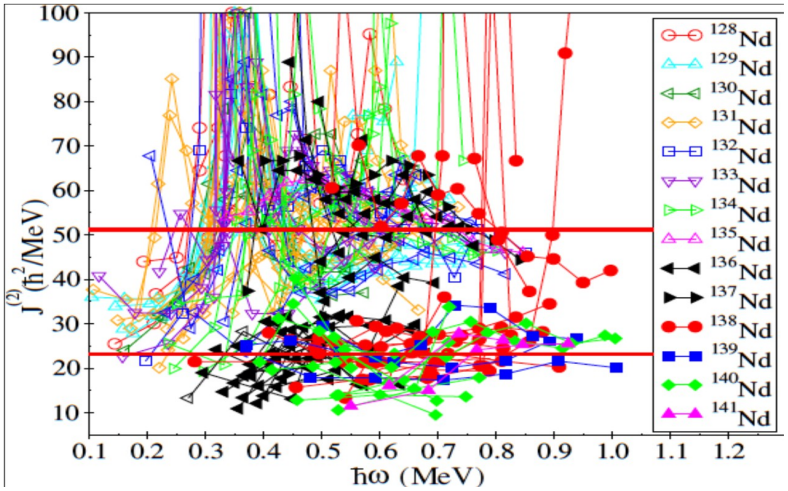

A possible explanation of the $\mathcal{J}^{(2)}$ gap in Fig. 1 is that in the light Nd nuclei the rotational bands have a large contribution from collective rotation which prefers the intermediate axis with maximum $\mathcal{J}^{(2)}$. On the contrary, in the heavy Nd nuclei the high-spin rotational bands have a large contribution from aligned particles, mainly from the $i_{13/2}$ and $f_{7/2}/h_{9/2}$ neutron orbitals from above N=82, which favors the rotation along the short axis. The moments of inertia associated to the two types of rotation appear to be different by a factor of two. For the ^{136,137,138}Nd nuclei there are bands built on configurations involving 1 or 2 neutrons in the strongly deformation driving $i_{13/2}$ orbital which induce larger $\mathcal{J}^{(2)}$ values than the other high-spin bands in these nuclei. The corresponding bands belong then to the group of nuclei with higher $\mathcal{J}^{(2)}$ and should be discussed separately. In the light $^{129-137}$Nd nuclei contributing to the group

As one can see in Fig. 1, the moments of inertia of the plotted bands in Nd nuclei lighter than ^{136}Nd are larger than those of the bands plotted for the heavier Nd nuclei. The average $\mathcal{J}^{(2)}$ for the light nuclei is $\approx$51 $\hbar^2$/MeV, which is nearly twice as large as the $\approx$23 $\hbar^2$/MeV value for the heavy nuclei. This behavior of $\mathcal{J}^{(2)}$ is somewhat surprising, since one would expect gradual decreasing values going from light to heavy nuclei, induced by the gradual decrease of the deformation when approaching the N=82 shell closure. The calculated shapes for the observed bands in the light Nd nuclei are triaxial with $\gamma < 0°$ (or equivalently, the nucleus rotates around the intermediate axis of the triaxial shape), while for the heavy Nd nuclei the calculated shapes are triaxial with $\gamma > 0°$ (or equivalently, the nucleus rotates around the short axis). As one can see in Fig. 1, in ^{136}Nd, ^{137}Nd and ^{138}Nd both types of bands are present: the $\mathcal{J}^{(2)}$ of the highly-deformed bands of ^{136}Nd, ^{137}Nd and ^{138}Nd belong to the group with high $\mathcal{J}^{(2)}$, while the other high-spin bands belong to the group with low $\mathcal{J}^{(2)}$. It seems that there is a sharp transition of the rotational regime at neutron number N=76-77, implying a switch of the rotation axis from intermediate to short when moving from light to heavy nuclei. Another feature clearly visible in Fig. 1 are the crossings observed in some bands of ^{138}Nd, namely in bands 1, 2, 7 and 8 [18, 20]. The crossings in the bands 1 and 2 has been interpreted using CNS calculations as the manifestation of a switch of the rotation axis from short to intermediate with increasing spin [18]. The
bands 7 and 8
caused by in
smaller ε_2 val

C. Petrache,
Phys. Scr. (2015)

Nd Nuclei

Intermediate axis

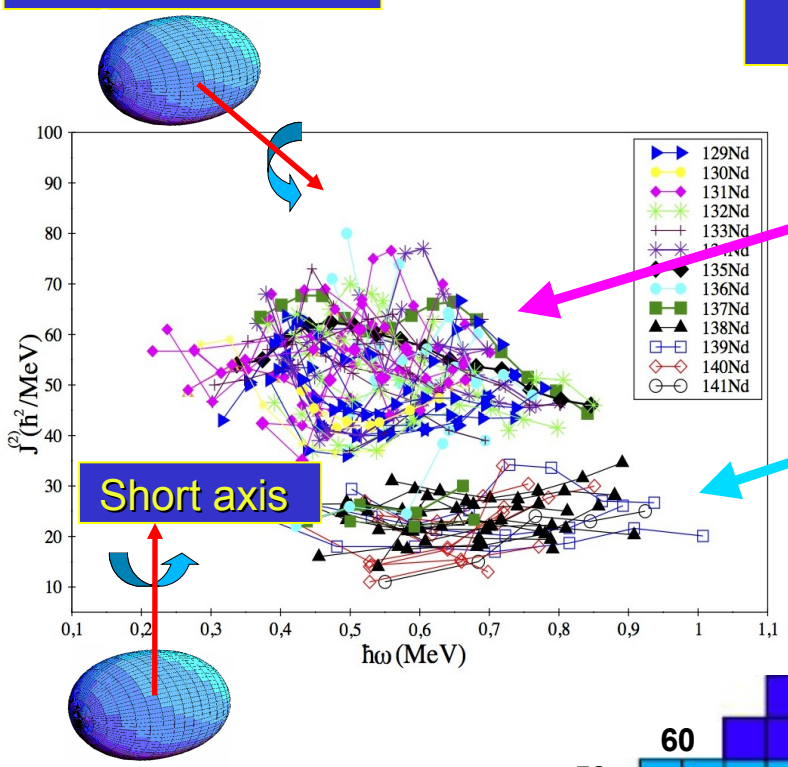

Short axis

^{133}Nd-^{136}Nd

^{138}Nd-^{141}Nd

66

60

59

58

57

56

55

50

50

64 66 68

82

Conclusions, perspectives

Many questions wait an answer :
- transverse wobbling in other nuclei with A=130-140
- transverse wobbling in other mass regions
- transverse wobbling in excited configurations
- precise measurement of transition probabilities
- precise measurement of mixing ratios
- comprehensive interpretation of the behaior of sequences of nuclei, like e.g. the Nd chain